Journal of Nonlinear Modeling and Analysis
Volume 7, Number 1, February 2025, 268–302
https://journal.global-sci.org/jnma
DOI:10.12150/jnma.2025.268

Numerical Approximation of the Fractional Pine Wilt Disease Model via Taylor Wavelet Collocation Method

Kumbinarasaiah S[1,†],Manohara G[1]

Abstract This article aims to develop a quick and easy Taylor wavelet collocation method with the help of an operational matrix of integration of the Taylor wavelets. Solving epidemiological models ensures the necessary accuracy for relatively small grid points. Finding the appropriate approximations with a new numerical design is challenging. This study examines the fractional Pine wilt disease (PWD) model. Using the Caputo fractional derivative for the fractional order, we developed the novel wavelet scheme known as the Taylor wavelet collocation technique (TWCM) to approximate the PWD model numerically. The results have been compared between the developed method, the Homotopy analysis transform method (HATM), the RK4 method, and the ND solver. The numerical outcomes demonstrate that (TWCM) is incredibly effective and precise for solving the PWD model of fractional order. The approach under consideration is a powerful tool for obtaining numerical solutions to fractional-order nonlinear differential equations. The fractional order differential operator provides a more advanced way to study the dynamic behavior of different complex systems than the integer order differential operator does. The proposed wavelet method suits solutions with sharp edge/ jump discontinuities. Fractional differential equations, delay differential equations, and stiff systems can be solved using this method directly without using any control parameters. For highly nonlinear problems, the TWCM technique yields accurate solutions close to exact solutions by avoiding data rounding and just computing a few terms. Mathematical software Mathematica has been used for numerical computations and implementation.

Keywords Taylor wavelet, Caputo fractional derivative (CFD), system of fractional ordinary differential equations (SFODEs), Pine wilt disease model

MSC(2010) 34A08, 34A34, 34K28, 78A70, 93A30.

1. Introduction

Mathematical modelling is a potent instrument for studying, investigating, and understanding the spread of various diseases and developing methods to manage them in society. Mathematical modelling makes understanding a disease's spread and defining the essential factors easier. Numerous biological models have been examined from different aspects in this regard. Infectious disease models for humans, animals, plants, and trees have all been developed in the literature. Forests are

[†]the corresponding author.
Email address: kumbinarasaiah@gmail.com
[1]Department of Mathematics, Bangalore University, Bengaluru-560 056, India

crucial to human life. Its significance is indescribable in words because a single forest can completely rejuvenate the planet. Consequently, it is essential to safeguard trees. In addition to creating a green carpet on Earth, trees give us access to necessities like clean air. Pine wilt disease (PWD) destroys trees within weeks of symptoms showing, despite its majestic and elegant appearance. The pathogens, which include bacteria, viruses, and protozoa, are the leading causes of infectious disorders [1, 2]. The average lifespan of pine trees with PWD infection is a few months. "Wilt diseases" refers to various ailments that affect a plant's vascular system. Plants can be attacked by nematodes, fungi, and bacteria, which instantly destroy them. Viruses can exist in plants as well. Two types of wilt diseases affect woody plants: those that start at the branches and those that begin at the roots. Only a small percentage of infections spread to other plants via the root grafting, typically starting at the stems, where pathogens feed on leaves or bark. Most infections start as lesioning or as pathogens entering the roots directly. The only way to protect the pine forest is to keep it free of disease, as diseased pine trees cannot be spared.

The following set of non-linear equations is used to describe the complex model [3,11,43,44]. $S(\xi)$, $E(\xi)$, $I(\xi)$, $R(\xi)$ and $R(\xi)$ are used to represent the susceptible pine tree class, exposed pine trees, infected pine trees, and susceptible beetle class, respectively. Additionally, $Q(\xi)$ represents the infectious class of beetles.

$$\left.\begin{aligned}
\tfrac{dS(\xi)}{d\xi} &= \theta - \delta\ S(\xi)\ Q(\xi)(1+\epsilon\ Q(\xi)) - \psi\ S(\xi),\\
\tfrac{dE(\xi)}{d\xi} &= \delta\ S(\xi)\ Q(\xi)\ (1+\epsilon\ Q(\xi)) - (\tau+\psi)\,E(\xi),\\
\tfrac{dI(\xi)}{d\xi} &= \tau\ E(\xi) - \psi\ I(\xi),\\
\tfrac{dR(\xi)}{d\xi} &= \lambda - a\ I(\xi)\,R(\xi)(1+\kappa\ I(\xi)) - \beta\ R(\xi),\\
\tfrac{dQ(\xi)}{d\xi} &= a\ I(\xi)\,R(\xi)(1+\kappa\ I(\xi)) - \beta\ Q(\xi).
\end{aligned}\right\} \tag{1.1}$$

The symbol θ denotes the entry of new trees into growth. New beetles entering induction are indicated by the symbol λ, and ψ denotes the ratio of dead trees to newly planted ones. Additionally, β reflects the beetle mortality rate, a represents the nematode growth rate, κ denotes the saturation of the beetle infection,ϵ is the infection saturation in trees, δ is the trees contact rate, and τ is the beetle contact rate. The initial conditions are $S(0) = 300$, $E(0) = 30$, $I(0) = 20$, $R(0) = 65$ and $Q(0) = 20$. The parametric values are $\theta = 0.009041, \delta = 0.00166$, $\epsilon = 0.01$, $\psi = 0.0000301$, $\tau = 0.002691$, $\lambda = 0.057142$, $a = 0.00305$, $\kappa = 0.02$, $\beta = 0.01176$.

The fractional mathematical model in Caputo fractional derivative: Now, we incorporate the fractional order into the ODE model. Since fractional calculus has received much attention from researchers lately, various elements of the topic are being considered for investigation. Creating mathematical models based on fractional differential equation and examining their dynamical behaviors are effective and valuable methods of understanding biological issues. The hereditary characteristics, system memory, and non-local distributed effects are all considered by fractional order derivatives and integrals.

Therefore, we modify the system by changing the time derivative with the CFD to present the influence of non-locality. The following fractional SODEs represent

the mathematical model of Pine wilt disease.

$$\left.\begin{aligned} D_{\xi}^{\alpha} S(\xi) &= \theta - \delta\ S(\xi) Q(\xi)(1+\epsilon\ Q(\xi)) - \psi\ S(\xi), \\ D_{\xi}^{\alpha} E(\xi) &= \delta\ S(\xi) Q(\xi)(1+\epsilon\ Q(\xi)) - (\tau+\psi) E(\xi), \\ D_{\xi}^{\alpha} I(\xi) &= \tau\ E(\xi) - \psi\ I(\xi), \\ D_{\xi}^{\alpha} R(\xi) &= \lambda - a\ I(\xi) R(\xi)(1+\kappa\ I(\xi)) - \beta\ R(\xi), \\ D_{\xi}^{\alpha} Q(\xi) &= a\ I(\xi) R(\xi)(1+\kappa\ I(\xi)) - \beta\ Q(\xi). \end{aligned}\right\} \tag{1.2}$$

With $0 < \alpha < 1$, the fractional derivative in the Caputo sense is denoted by D_{ξ}^{α}.

Several researchers have examined the various PWD facets. The pathophysiology and history of PWD, brought on by Bursaphelenchus xylophilus, were covered by Mamiya [4, 5]. Fukuda [6] used pathological studies in 1997 to investigate conceptual functions associated with the progression or inhibition of PWD. Proenca et al. [7] described the characteristics of the bacteria the pinewood nematode carries to understand PWD better. The model was examined by Ozair et al. [8] using Biostimulated analytical heuristics. Numerical modelling and symmetry investigation of a model were carried out by Padmavathi et al. [9]. Yongjin Li et al. initiated the LADM for the PWD model [10,11]. Kamal Shah et al. conducted a semi-analytical investigation on the PWD [3]. The N-ADM and fractional Euler methods were applied by El-Sayed et al. [12]. Dynamic aspects of the PWD model were examined by Hussain T et al. [13]. In their studies, over the last few decades, many researchers have covered a stability analysis of PWD and its causes [14, 15].

A recent and promising development in mathematics is wavelet theory. It has been applied in many fields, such as biological field, time-frequency analysis, signal analysis for waveform representation and segmentation, and rapid techniques for simple implementation. The properties of wavelet methods, such as their orthogonality, compact support, and ability to accurately represent a range of functions and operators at different resolution levels, have drawn much interest in the last three decades for the numerical solution of differential equations. An orthogonal family of functions has been widely employed to approximate solutions to many dynamical system problems. The integral operations can then be eliminated using the operational integration matrix. Despite not being constructed on orthogonal functions, the Taylor series and Fibonacci polynomials possess the operational integration matrix. Another benefit of using an orthogonal wavelet basis over traditional methods is multi-resolution analysis. Numerous wavelet collocation techniques, including the Hermite wavelet collocation method [16], the Laguerre wavelet collocation method [17], the Bernoulli and Gegenbauer wavelet collocation method [18, 19], and the Chebyshev wavelet collocation method [20], have been applied to some common mathematical problems. Fractional differential equations are typically solved using a variety of wavelet collocation techniques, such as Hermite wavelets [21, 22], Cubic B Spline [23], Chebyshev wavelets [24], Genocchi wavelets [25], Bernoulli wavelets [26–28], Haar wavelets [29], Chelyshkov wavelets [30], Fibonacci wavelets [31, 32], Legendre wavelet tau method [33], and Legendre wavelets and Gegenbaur wavelets [34].

In the article [25], author Abdulnasir Isah et al. implemented the Genocchi wavelets operational matrix technique to solve the nonlinear fractional differential equation (FDEs). The Genocchi wavelet collocation method is developed with the help of an operational matrix of integration. The numerical solution is obtained for different examples of nonlinear FDEs and compared with the various techniques

available in the literature. In the article [27], author Kumbinarasaiah et al. proposed the Bernoulli wavelets functional matrix technique to solve the nonlinear singular Lane-Emden equation system. Initially, a functional matrix of integration (FMI) was extracted using Bernoulli wavelets. Later on, with the help of FMI, the Bernoulli wavelet collocation method was implemented, and the numerical approximation for the nonlinear singular Lane-Emden equation system was obtained. In the article [28], author Kumbinarasaiah et al. proposed a similar Bernoulli wavelets functional matrix technique to solve the biological model (HIV infection of CD4+ T cells model). In both articles, the author obtained a numerical approximation that is very close to the actual solutions and compared it with the existing techniques available in the literature to show the methods' accuracy and efficiency.

The ongoing effort aims to develop a quick and easy Taylor wavelets collocation method. Solving epidemiological models ensures the necessary accuracy for relatively small grid points. Finding the appropriate approximations with a new numerical design is challenging. The Taylor wavelets, created by Taylor polynomials, are a recent addition to the wavelet family. Recently, there has been an increased focus on wavelet techniques for solving differential and integral equations. Mathematical problems such as Burger's equation [35], Bratu-type equations [36], linear and nonlinear Lane-Emden equations [37], fractional delay differential equations [38], Benjamin-Bona-Mohany PDEs [39], and systems of nonlinear FDEs with application to HRS virus infection [40], are among some of the problems that researchers have used this package to solve [42–45]. Some of the articles utilized to improve the paper are listed below.

Splines solutions of boundary value problems [46], an innovative Fibonacci wavelet collocation method for the numerical approximation of Emden-Fowler equations [47], an approximate analytical view of physical and biological models in the setting of Caputo operator via Elzaki transform decomposition method [48], an efficient variable stepsize rational method for stiff, singular and singularly perturbed problems [49], a study on fractional HIV-AIDs transmission model with awareness effect [50], numerical approximation of fractional SEIR epidemic model of measles and smoking model by using Fibonacci wavelets operational matrix approach [51], a numerical combined algorithm in cubic B-spline method and finite difference technique for the time-fractional nonlinear diffusion wave equation with reaction and damping terms [52], the novel cubic B-spline method for fractional Painleve and Bagley-Trovik equations in the Caputo, Caputo-Fabrizio, and conformable fractional sense [53], cubic splines solutions of the higher order boundary value problems arising in sandwich panel theory [54], numerical approximation of the typhoid disease model via Genocchi wavelet collocation method [55], a new adaptive nonlinear numerical method for singular and stiff differential problems [56], and extracting the Ultimate New Soliton Solutions of Some Nonlinear Time Fractional PDEs via the Conformable Fractional Derivative [57]. The ongoing effort of this article aims to develop a quick and easy Taylor wavelets collocation method. Solving epidemiological models ensures the necessary accuracy for relatively small grid points. Finding the appropriate approximations with a new numerical design is challenging. The system's solution was significantly approximated after applying the Taylor wavelet collocation technique. Currently, no one has been able to solve the fractional pine wilt disease model using Taylor wavelets, which encourages us to investigate this using the established method.

Here's how this article is organized: Wavelet definitions can be found in Section

2. In Section 3, the FMI of Taylor wavelets has been carried out. Sections 4 and 5, respectively, we describe the method of solution and numerical illustration of the method. The conclusion is finally given in Section 6.

2. Fractional derivative and Taylor wavelets

Definition 2.1. Caputo fractional derivative

The Caputo fractional derivative of $f(\xi) \in C\mu$ is defined as [41]:

$$\frac{d^{\alpha} f(\xi)}{ds^{\alpha}} = \frac{1}{\Gamma(m-\alpha)} \int_0^{\xi} (\xi - t)^{m-\alpha-1} f^{(m)}(t)\, dt.$$

For $m-1 < \alpha \leq m$, m is any positive integer, $\xi > 0$, $f(\xi) \in C_{\mu}^{m}$, $\mu \geq -1$.

Definition 2.2. Taylor wavelets

On the interval [0,1], the Taylor wavelets are defined as [35],

$$\Upsilon_{n,m}(\xi) = \begin{cases} 2^{\frac{k-1}{2}} T_m\left(2^{k-1}\xi - n + 1\right), & \frac{n-1}{2^{k-1}} \leq \xi < \frac{n}{2^{k-1}}, \\ 0, & \text{Otherwise}, \end{cases}$$

where $T_m(\xi) = \sqrt{2m+1}\,\xi^m$,
where $T_m(\xi)$ is the normal Taylor polynomial of degree m, translation parameter $n = 1, 2, \ldots, 2^{k-1}$ and, k represents the level of resolution $k = 1, 2, \ldots$ and respectively. Taylor wavelets are compactly supported wavelets formed by Taylor polynomials over the interval [0,1].

Theorem 2.1. *[41] Let $L^2[0,1]$ be the Hilbert space generated by the Taylor wavelet basis. Let $\eta(\xi)$ be the continuous bounded function in $L^2[0,1]$. Then, the Taylor wavelet expansion of $\eta(\xi)$ converges with it.*

Proof. Let $\eta : [0,1] \to R$ be a continuous function and $|\eta(\xi)| \leq \mu$, where μ is any real number. Then Taylor wavelet dilation of $\eta(\xi)$ can be expressed as,

$$\eta(\xi) = \sum_{n=1}^{2^{\frac{k-1}{2}}} \sum_{m=0}^{M-1} a_{n,m} \Upsilon_{n,m}(\xi),$$

where $a_{n,m} = \langle\, \eta(\,\xi\,),\, \Upsilon_{n,m}(\xi) \rangle$ denotes inner product.

$$a_{n,m} = \int_0^1 \eta(\xi)\, \Upsilon_{n,m}(\xi)\, d\xi.$$

Since $\Upsilon_{n,m}$ are the orthogonal basis,
$a_{n,m} = \int_I \eta\,(\xi) T_m\left(2^{k-1}\xi - n + 1\right)\, d\xi$ where $I = \left[\frac{n-1}{2^{k-1}}\,,\ \frac{n}{2^{k-1}}\right)$.
Since $T_m(\xi) = \sqrt{2m+1}\,\xi^m$, we obtain,
$a_{n,m} = \int_I \eta\,(\xi)\,\sqrt{2m+1}\,\left(2^{k-1}\xi - n + 1\right)^m d\xi$ where $I = \left[\frac{n-1}{2^{k-1}}\,,\ \frac{n}{2^{k-1}}\right)$.
Substitute $2^{k-1}\xi - n + 1 = y$. Then, we get,

$$a_{n,m} = \frac{2^{\frac{k-1}{2}}}{\sqrt{2m+1}} \int_0^1 \eta\left(\frac{y + n - 1}{2^{k-1}}\right) y^m \frac{dy}{2^{k-1}},$$

$$a_{n,m} = \frac{2^{\frac{1-k}{2}}}{\sqrt{2m+1}} \int_{.0}^{1} \eta\left(\frac{y \ + \ n-1}{2^{\,k-1}}\right) y^m \, dy.$$

By generalized mean value theorem,

$$a_{n,m} \ = \frac{2^{\frac{-k+1}{2}}}{\sqrt{2m+1}} \, \eta\left(\frac{\delta+n-1}{2^{\,k-\,1}}\right) \int_0^1 \ y^m \ dy \text{ for some } \delta \in (0,1).$$

Since y^m is a bounded continuous function, put $\int_0^1 \ y^m \ dy = h$,

$$|a_{n,m}| \ = \left|\frac{2^{\frac{-k+1}{2}}}{\sqrt{2m+1}}\right| \left|\eta\left(\frac{\delta+n-\ 1}{2^{k-1}}\right)\right| \ h.$$

Since η remains bounded,

Hence, $|a_{n,m}| \ = \left|\frac{2^{\frac{-k+1}{2}}}{\sqrt{2m+1}} \ \mu \ h\right|$ where $\mu = \eta\left(\frac{\delta+n-\ 1}{2^{k-1}}\right)$.

Therefore, $\sum_{n,m=0}^{\infty} a_{n,m}$ is absolutely convergent. Hence, the Taylor wavelet series expansion $\eta(\xi)$ converges uniformly to it. □

Theorem 2.2. *[41] Let $I \subset R$ be a finite interval with length $m(I)$. Furthermore, $f(\xi)$ is an integrable function defined on I and $\sum_{i=0}^{M-1} \sum_{j=1}^{2^{k-1}} a_{i,j} \Upsilon_{i,j}(\xi)$ be a good Taylor wavelet approximation of f on I. For some $\epsilon > 0$, $\left|f(\xi) - \sum_{i=0}^{M-1} \sum_{j=1}^{2^{k-1}} a_{i,j} \Upsilon_{i,j}(\xi)\right| \leq \epsilon, \ \forall \ x \in I$. Then $-\epsilon \, m(I) + \int_I \sum \sum a_{i,j} \Upsilon_{i,j}(\xi) \, d\xi \leq \int_I f(\xi) \, d\xi \leq \epsilon \, m(I) + \int_I \sum \sum a_{i,j} \ \Upsilon_{i,j}(\xi) \ d\xi$.*

3. Operational matrix of integration (OMI)

The following are the computed Taylor wavelet basis (TWB) at $k = 1$ and $M = 6$.

$$\begin{aligned}
\Upsilon_{1,0}(\xi) &= 1, \\
\Upsilon_{1,1}(\xi) &= \sqrt{3}\xi, \\
\Upsilon_{1,2}(\xi) &= \sqrt{5}\xi^2, \\
\Upsilon_{1,3}(\xi) &= \sqrt{7}\xi^3, \\
\Upsilon_{1,4}(\xi) &= 3\xi^4, \\
\Upsilon_{1,5}(\xi) &= \sqrt{11}\xi^5, \\
\Upsilon_{1,6}(\xi) &= \sqrt{13}\xi^6, \\
\Upsilon_{1,7}(\xi) &= \sqrt{15}\xi^7.
\end{aligned}$$

After integrating the first six bases mentioned above concerning the limit ξ between 0 and ξ, and expressing the Taylor wavelet bases as a linear combination, we obtain,

$$\int_0^{\xi} \Upsilon_{1,0}(\xi) \, d\xi = \left[0 \ \tfrac{1}{\sqrt{3}} \ 0 \ 0 \ 0 \ 0\right] \ \Upsilon_6(\xi),$$

$$\int_0^{\xi} \Upsilon_{1,1}(\xi) \, d\xi = \left[0 \ 0 \ \tfrac{\sqrt{\frac{3}{5}}}{2} \ 0 \ 0 \ 0\right] \Upsilon_6(\xi),$$

$$\int_0^{\xi} \Upsilon_{1,2}(\xi)\, d\xi = \left[0\ 0\ 0\ \tfrac{\sqrt{\frac{5}{7}}}{3}\ 0\ 0\right] \Upsilon_6(\xi),$$
$$\int_0^{\xi} \Upsilon_{1,3}(\xi)\, d\xi = \left[0\ 0\ 0\ 0\ \tfrac{\sqrt{7}}{12}\ 0\right] \Upsilon_6(\xi),$$
$$\int_0^{\xi} \Upsilon_{1,4}(\xi)\, d\xi = \left[0\ 0\ 0\ 0\ 0\ \tfrac{3}{5\sqrt{11}}\right] \Upsilon_6(\xi),$$
$$\int_0^{\xi} \Upsilon_{1,5}(\xi)\, d\xi = \left[0\ 0\ 0\ 0\ 0\ 0\right]\ \Upsilon_6(\xi),$$
$$\int_0^{\delta} \Upsilon(\xi)\ d\xi = \mathcal{B}_{6\times 6}\Upsilon_6\ (\xi)\ + \overline{\Upsilon}_6(\xi), \tag{3.1}$$

where

$$\Upsilon_6(\xi) = [\Upsilon_{1,0}(\xi),\ \Upsilon_{1,1}(\xi), \Upsilon_{1,2}(\xi),\ \Upsilon_{1,3}(\xi), \Upsilon_{1,4}(\xi), \Upsilon_{1,5}(\xi)]^T,$$

$$\mathcal{B}_{6\times 6} = \begin{bmatrix} 0 & \frac{1}{\sqrt{3}} & 0 & 0 & 0 & 0 \\ 0 & 0 & \frac{\sqrt{\frac{3}{5}}}{2} & 0 & 0 & 0 \\ 0 & 0 & 0 & \frac{\sqrt{\frac{5}{7}}}{3} & 0 & 0 \\ 0 & 0 & 0 & 0 & \frac{\sqrt{7}}{12} & 0 \\ 0 & 0 & 0 & 0 & 0 & \frac{3}{5\sqrt{11}} \\ 0 & 0 & 0 & 0 & 0 & 0 \end{bmatrix}, \overline{\Upsilon}_6(\xi) = \begin{bmatrix} 0 \\ 0 \\ 0 \\ 0 \\ 0 \\ \frac{\sqrt{\frac{11}{13}}}{6}\Upsilon_{1,6}(\xi) \end{bmatrix}.$$

Defined as follows, the generalized OMI of the $n-$wavelet basis is

$$\int_0^{\xi} \Upsilon\ (\xi)\, d\xi = \mathcal{B}_{n\times n}\Upsilon(\xi) + \overline{\Upsilon}_n(\xi),$$

where

$$\mathcal{B}_{n\times n} = \begin{bmatrix} 0 & \frac{1}{\sqrt{3}} & 0 & 0 & 0 & \dots & 0 & 0 \\ 0 & 0 & \frac{\sqrt{\frac{3}{5}}}{2} & 0 & 0 & \dots & 0 & 0 \\ 0 & 0 & 0 & 0 & \frac{\sqrt{7}}{12} & \dots & 0 & 0 \\ \vdots & \vdots & \vdots & \vdots & \vdots & \dots & 0 & 0 \\ 0 & 0 & 0 & 0 & 0 & \dots & \frac{\sqrt{2(n-2)+1}}{(n-1)\sqrt{2(n-2)+3}} & 0 \\ 0 & 0 & 0 & 0 & 0 & \dots & 0 & \frac{\sqrt{2(n-1)+1}}{n\sqrt{2(n-1)+3}} \\ 0 & 0 & 0 & 0 & 0 & \dots & 0 & 0 \end{bmatrix}, \overline{\Upsilon}_n(\xi) = \begin{bmatrix} 0 \\ 0 \\ 0 \\ 0 \\ 0 \\ 0 \\ \vdots \\ \frac{\sqrt{2n-1}}{n\sqrt{2n+1}}\Upsilon_{1,n}(\xi) \end{bmatrix}.$$

Integrating the previously mentioned bases once again yields the following results:

$$\int_0^{\xi}\int_0^{\xi} \Upsilon_{1,0}(\xi)\ d\xi = \left[0\ 0\ \tfrac{1}{2\sqrt{5}}\ 0\ 0\ 0\right] \Upsilon_6(\xi),$$
$$\int_0^{\xi}\int_0^{\xi} \Upsilon_{1,1}(\xi)\ d\xi = \left[0\ 0\ 0\ \tfrac{1}{2\sqrt{21}}\ 0\ 0\right] \Upsilon_6(\xi),$$

$$\int_0^\xi \int_0^\xi \Upsilon_{1,2}(\xi)\ d\xi = \left[0\ 0\ 0\ 0\ \tfrac{\sqrt{5}}{36}\ 0\right] \Upsilon_6(\xi),$$
$$\int_0^\xi \int_0^\xi \Upsilon_{1,3}(\xi)\ d\xi = \left[0\ 0\ 0\ 0\ 0\ \tfrac{\sqrt{\frac{7}{11}}}{20}\right] \Upsilon_6(\xi),$$
$$\int_0^\xi \int_0^\xi \Upsilon_{1,4}(\xi)\ d\xi = \left[0\ 0\ 0\ 0\ 0\ 0\right] \Upsilon_6(\xi),$$
$$\int_0^\xi \int_0^\xi \Upsilon_{1,5}(\xi)\ d\xi = \left[0\ 0\ 0\ 0\ 0\ 0\right] \Upsilon_6(\xi).$$

Hence,

$$\int_0^\xi \int_0^\xi \Upsilon(\xi)\ d\xi = \mathcal{B}'_{6\times 6}\Upsilon_6(\xi) + \overline{\Upsilon}'_6(\xi), \tag{3.2}$$

where $\Upsilon_6(\xi) = [\Upsilon_{1,0}(\xi),\ \Upsilon_{1,1}(\xi), \Upsilon_{1,2}(\xi),\ \Upsilon_{1,3}(\xi), \Upsilon_{1,4}(\xi), \Upsilon_{1,5}(\xi)]^T$,

$$\mathcal{B}'_{6\times 6} = \begin{bmatrix} 0 & 0 & \frac{1}{2\sqrt{5}} & 0 & 0 & 0 \\ 0 & 0 & 0 & \frac{1}{2\sqrt{21}} & 0 & 0 \\ 0 & 0 & 0 & 0 & \frac{\sqrt{5}}{36} & 0 \\ 0 & 0 & 0 & 0 & 0 & 0\frac{\sqrt{\frac{7}{11}}}{20} \\ 0 & 0 & 0 & 0 & 0 & 0 \\ 0 & 0 & 0 & 0 & 0 & 0 \end{bmatrix}, \overline{\Upsilon}'_6(\xi) = \begin{bmatrix} 0 \\ 0 \\ 0 \\ 0 \\ \frac{1}{10\sqrt{13}}\ \Upsilon_{1,6}(\xi) \\ \frac{\sqrt{\frac{11}{15}}}{42}\ \Upsilon_{1,7}(\xi) \end{bmatrix}.$$

At $k = 2$ and $M = 6$, the TWB is investigated as follows:

$$\left.\begin{aligned} \Upsilon_{1,0}(\xi) &= \sqrt{2}, \\ \Upsilon_{1,1}(\xi) &= 2\sqrt{6}\ \xi, \\ \Upsilon_{1,2}(\xi) &= 4\sqrt{10}\ \xi^2, \\ \Upsilon_{1,3}(\xi) &= 8\sqrt{14}\ \xi^3, \\ \Upsilon_{1,4}(\xi) &= 48\sqrt{2}\ \xi^4, \\ \Upsilon_{1,5}(\xi) &= 32\sqrt{22}\ \xi^5. \end{aligned}\right\} \quad 0 \le \xi < \frac{1}{2},$$

$$\left.\begin{aligned}
&\Upsilon_{2,0}(\xi) = \sqrt{2},\\
&\Upsilon_{2,1}(\xi) = \sqrt{6}(-1+2\,\xi),\\
&\Upsilon_{2,2}(\xi) = \sqrt{10}(1-2\,\xi)^2,\\
&\Upsilon_{2,3}(\xi) = \sqrt{14}(-1+2\,\xi)^3,\\
&\Upsilon_{2,4}(\xi) = 3\sqrt{2}(1-2\,\xi)^4,\\
&\Upsilon_{2,5}(\xi) = \sqrt{22}(-1+2\,\xi)^5,
\end{aligned}\right\} \qquad \frac{1}{2} \le \xi < 1,$$

$$\int_0^{\xi} \Upsilon(\xi)\, d\xi = \mathcal{B}_{12\times 12}\, \Upsilon_{12}(\xi) + \overline{\Upsilon}_{12}(\xi). \tag{3.3}$$

$$\Upsilon_{12}(\xi) = [\Upsilon_{1,0}(\xi), \Upsilon_{1,1}(\xi), \Upsilon_{1,2}(\xi), \Upsilon_{1,3}(\xi), \Upsilon_{1,4}(\xi), \Upsilon_{1,5}(\xi), \Upsilon_{2,0}(\xi), \Upsilon_{2,1}(\xi), \Upsilon_{2,2}(\xi), \Upsilon_{2,3}(\xi), \Upsilon_{2,4}(\xi), \Upsilon_{2,5}(\xi)]^T,$$

$$\mathcal{B}_{12\times 12} = \begin{bmatrix}
0 & \frac{1}{2\sqrt{3}} & 0 & 0 & 0 & 0 & 0 & 0 & 0 & 0 & 0 & 0\\
0 & 0 & \frac{\sqrt{\frac{3}{5}}}{4} & 0 & 0 & 0 & 0 & 0 & 0 & 0 & 0 & 0\\
0 & 0 & 0 & \frac{\sqrt{\frac{5}{7}}}{6} & 0 & 0 & 0 & 0 & 0 & 0 & 0 & 0\\
0 & 0 & 0 & 0 & \frac{\sqrt{\frac{31}{34}}}{6} & 0 & 0 & 0 & 0 & 0 & 0 & 0\\
0 & 0 & 0 & 0 & 0 & \frac{3}{10\sqrt{11}} & 0 & 0 & 0 & 0 & 0 & 0\\
0 & 0 & 0 & 0 & 0 & 0 & 0 & 0 & 0 & 0 & 0 & 0\\
0 & 0 & 0 & 0 & 0 & 0 & 0 & \frac{1}{2\sqrt{3}} & 0 & 0 & 0 & 0\\
0 & 0 & 0 & 0 & 0 & 0 & 0 & 0 & \frac{\sqrt{\frac{3}{5}}}{4} & 0 & 0 & 0\\
0 & 0 & 0 & 0 & 0 & 0 & 0 & 0 & 0 & \frac{\sqrt{\frac{5}{7}}}{6} & 0 & 0\\
0 & 0 & 0 & 0 & 0 & 0 & 0 & 0 & 0 & 0 & \frac{\sqrt{7}}{24} & 0\\
0 & 0 & 0 & 0 & 0 & 0 & 0 & 0 & 0 & 0 & 0 & \frac{3}{10\sqrt{11}}\\
0 & 0 & 0 & 0 & 0 & 0 & 0 & 0 & 0 & 0 & 0 & 0
\end{bmatrix},$$

and

$$\overline{\Upsilon}_{12}(\xi) = \begin{bmatrix} 0 \\ 0 \\ 0 \\ 0 \\ 0 \\ \frac{\sqrt{\frac{11}{13}}}{12}\Upsilon_{1,6}(\xi) \\ 0 \\ 0 \\ 0 \\ 0 \\ 0 \\ \frac{\sqrt{\frac{11}{13}}}{12}\Upsilon_{2,6}(\xi) \end{bmatrix}.$$

At $k = 2$, the generalized first integration of the $n-$wavelet basis is defined as follows:

$$\int_0^{\xi} \Upsilon(\xi)\, d\xi = \mathcal{B}_{2n\times 2n}\Upsilon(\xi) + \overline{\Upsilon}_{2n}(\xi) \ ,$$

where

$$\mathcal{B}_{2n\times 2n} = \begin{bmatrix}
0 & \frac{1}{2\sqrt{3}} & 0 & 0 & 0 & \dots & 0 & 0 & 0 & 0 & 0 & 0 & 0 & 0 & 0 & 0 \\
0 & 0 & \frac{\sqrt{\frac{3}{5}}}{4} & 0 & 0 & \dots & 0 & 0 & 0 & 0 & 0 & 0 & 0 & 0 & 0 & 0 \\
0 & 0 & 0 & \frac{\sqrt{\frac{5}{7}}}{6} & 0 & \dots & 0 & 0 & 0 & 0 & 0 & 0 & 0 & 0 & 0 & 0 \\
0 & 0 & 0 & 0 & \frac{\sqrt{7}}{24} & \dots & 0 & 0 & 0 & 0 & 0 & 0 & 0 & 0 & 0 & 0 \\
\vdots & \vdots & \vdots & \vdots & \vdots & \dots & 0 & 0 & 0 & 0 & 0 & 0 & 0 & 0 & 0 & 0 \\
0 & 0 & 0 & 0 & 0 & \dots & \frac{\sqrt{2(n-2)+1}}{(2n-1)\sqrt{2(n-2)+3}} & 0 & 0 & 0 & 0 & 0 & 0 & 0 & 0 & 0 \\
0 & 0 & 0 & 0 & 0 & 0 & 0 & \frac{\sqrt{2(n-1)+1}}{2n\sqrt{2(n-1)+3}} & 0 & 0 & 0 & 0 & 0 & 0 & 0 & 0 \\
0 & 0 & 0 & 0 & 0 & 0 & 0 & 0 & 0 & 0 & 0 & 0 & 0 & 0 & 0 & 0 \\
0 & 0 & 0 & 0 & 0 & 0 & 0 & 0 & 0 & \frac{1}{2\sqrt{3}} & 0 & 0 & 0 & \dots & 0 & 0 \\
0 & 0 & 0 & 0 & 0 & 0 & 0 & 0 & 0 & 0 & \frac{\sqrt{\frac{3}{5}}}{4} & 0 & 0 & \dots & 0 & 0 \\
0 & 0 & 0 & 0 & 0 & 0 & 0 & 0 & 0 & 0 & 0 & \frac{\sqrt{\frac{5}{7}}}{6} & 0 & \dots & 0 & 0 \\
0 & 0 & 0 & 0 & 0 & 0 & 0 & 0 & 0 & 0 & 0 & 0 & \frac{\sqrt{7}}{24} & \dots & 0 & 0 \\
0 & 0 & 0 & 0 & 0 & 0 & 0 & 0 & 0 & \vdots & \vdots & \vdots & \vdots & \dots & 0 & 0 \\
0 & 0 & 0 & 0 & 0 & 0 & 0 & 0 & 0 & 0 & 0 & 0 & 0 & \dots & \frac{\sqrt{2(n-2)+1}}{(2n-1)\sqrt{2(n-2)+3}} & 0 \\
0 & 0 & 0 & 0 & 0 & 0 & 0 & 0 & 0 & 0 & 0 & 0 & 0 & 0 & 0 & \frac{\sqrt{2(n-1)+1}}{2n\sqrt{2(n-1)+3}}
\end{bmatrix},$$

$$\overline{\Upsilon}_{2n}(\xi) = \begin{bmatrix} 0 \\ 0 \\ 0 \\ 0 \\ 0 \\ \vdots \\ \frac{\sqrt{2n-1}}{2n\sqrt{2n+1}}\ \Upsilon_{1,n}(\xi) \\ 0 \\ 0 \\ 0 \\ 0 \\ 0 \\ \vdots \\ \frac{\sqrt{2n-1}}{2n\sqrt{2n+1}}\ \Upsilon_{2,n}(\xi) \end{bmatrix}.$$

Similar to the first integration, the second integration can be expressed as:

$$\int_0^{\xi}\int_0^{\xi} \Upsilon(\xi)\, d\xi d\xi = \mathcal{B}'_{12\times 12}\ \Upsilon_{12}(\xi) + \overline{\Upsilon'}_{12}(\xi), \tag{3.4}$$

where $\Upsilon_{12}(\xi) = [\Upsilon_{1,0}(\xi), \Upsilon_{1,1}(\xi), \Upsilon_{1,2}(\xi), \Upsilon_{1,3}(\xi), \Upsilon_{1,4}(\xi), \Upsilon_{1,5}(\xi), \Upsilon_{2,0}(\xi), \Upsilon_{2,1}(\xi), \Upsilon_{2,2}(\xi), \Upsilon_{2,3}(\xi), \Upsilon_{2,4}(\xi), \Upsilon_{2,5}(\xi)]^T$.

$$\mathcal{B}'_{12\times 12} = \begin{bmatrix} 0\,0 & \frac{1}{8\sqrt{5}} & 0 & 0 & 0 & 0\,0 & 0 & 0 & 0 & 0 \\ 0\,0 & 0 & \frac{1}{8\sqrt{21}} & 0 & 0 & 0\,0 & 0 & 0 & 0 & 0 \\ 0\,0 & 0 & 0 & \frac{\sqrt{5}}{144} & 0 & 0\,0 & 0 & 0 & 0 & 0 \\ 0\,0 & 0 & 0 & 0 & \frac{\sqrt{\frac{7}{11}}}{80} & 0\,0 & 0 & 0 & 0 & 0 \\ 0\,0 & 0 & 0 & 0 & 0 & 0\,0 & 0 & 0 & 0 & 0 \\ 0\,0 & 0 & 0 & 0 & 0 & 0\,0 & 0 & 0 & 0 & 0 \\ 0\,0 & 0 & 0 & 0 & 0 & 0\,0 & \frac{1}{8\sqrt{5}} & 0 & 0 & 0 \\ 0\,0 & 0 & 0 & 0 & 0 & 0\,0 & 0 & \frac{1}{8\sqrt{21}} & 0 & 0 \\ 0\,0 & 0 & 0 & 0 & 0 & 0\,0 & 0 & 0 & \frac{\sqrt{5}}{144} & 0 \\ 0\,0 & 0 & 0 & 0 & 0 & 0\,0 & 0 & 0 & 0 & \frac{\sqrt{\frac{7}{11}}}{80} \\ 0\,0 & 0 & 0 & 0 & 0 & 0\,0 & 0 & 0 & 0 & 0 \\ 0\,0 & 0 & 0 & 0 & 0 & 0\,0 & 0 & 0 & 0 & 0 \end{bmatrix}, \quad \text{and}$$

$$\overline{\Upsilon'}_{12}(\xi) = \begin{bmatrix} 0 \\ 0 \\ 0 \\ 0 \\ \frac{1}{40\sqrt{13}}\Upsilon_{1,6}(\xi) \\ \frac{\sqrt{\frac{11}{15}}}{168}\Upsilon_{1,7}(\xi) \\ 0 \\ 0 \\ 0 \\ 0 \\ \frac{1}{40\sqrt{13}}\Upsilon_{2,6}(\xi) \\ \frac{\sqrt{\frac{11}{15}}}{168}\Upsilon_{2,7}(\xi) \end{bmatrix}.$$

Similarly, we can create matrices at our convenience.

4. Taylor wavelet collocation method (TWCM)

The mathematical model of pine wilt disease is represented as an ODE system, and its solution via TWCM is explained in this section.

Assume that,

$$\left.\begin{aligned} \tfrac{dS(\xi)}{d\xi} &= A^T\ \Upsilon(\xi), \\ \tfrac{dE(\xi)}{d\xi} &= B^T\ \Upsilon(\xi), \\ \tfrac{dI(\xi)}{d\xi} &= C^T\ \Upsilon(\xi), \\ \tfrac{dR(\xi)}{d\xi} &= D^T\ \Upsilon(\xi), \\ \tfrac{dQ(\xi)}{d\xi} &= E^T\ \Upsilon(\xi), \end{aligned}\right\} \tag{4.1}$$

where
$A^T = [a_{1,1}, \ldots, a_{1,M}, a_{2,1}, \ldots, a_{2,M},\ a_{2^{k-1},1}, \ldots, a_{2^{k-1},M}]$,
$B^T = [b_{1,1}, \ldots, b_{1,M}, b_{2,1}, \ldots, b_{2,M},\ b_{2^{k-1},1}, \ldots, b_{2^{k-1},M}]$,
$C^T = [c_{1,1}, \ldots, c_{1,M}, c_{2,1}, \ldots, c_{2,M}, c_{2^{k-1},1}, \ldots, c_{2^{k-1},M}]$,
$D^T = [d_{1,1}, \ldots, d_{1,M}, d_{2,1}, \ldots, d_{2,M},\ d_{2^{k-1},1}, \ldots, d_{2^{k-1},M}]$,
$E^T = [e_{1,1}, \ldots, e_{1,M}, e_{2,1}, \ldots, e_{2,M},\ e_{2^{k-1},1}, \ldots, e_{2^{k-1},M}]$,

$\Upsilon(\xi) = [\Upsilon(\xi)_{1,0}, \ldots, \Upsilon(\xi)_{1,M-1}, \Upsilon(\xi)_{2,0}, \ldots \Upsilon(\xi)_{2,M-1}, \Upsilon(\xi)_{2^{k-1},0}, \ldots \Upsilon(\xi)_{2^{k-1},M-1}]$.

Equation (4.1) is about 'ξ' from '0' to 'ξ'. We get

$$\begin{aligned} S(\xi) &= S(0) + \int_0^{\xi} A^T \Upsilon(\xi)\, d\xi, \\ E(\xi) &= E(0) + \int_0^{\xi} B^T \Upsilon(\xi)\, d\xi, \\ I(\xi) &= I(0) + \int_0^{\xi} C^T \Upsilon(\xi)\, d\xi, \\ R(\xi) &= R(0) + \int_0^{\xi} D^T \Upsilon(\xi)\, d\xi, \\ Q(\xi) &= Q(0) + \int_0^{\xi} E^T \Upsilon(\xi)\, d\xi. \end{aligned}$$

Using equation (3.1) and primary constraints $S(0) = S_0$, $E(0) = E_0$, $I(0) = I_0$, $R(0) = R_0$ and $Q(0) = Q_0$ described regarding $\Upsilon(\xi)$ as $S(0) = F^T\ \Upsilon(\xi)$, $E(0) = G^T\ \Upsilon(\xi)$, $I(0) = H^T\ \Upsilon(\xi)$, $R(0) = K^T\ \Upsilon(\xi)$ and $Q(0) = L^T\ \Upsilon(\xi)$, we obtain

$$\left.\begin{aligned} \mathcal{S}(\xi) &= F^T\Upsilon(\xi) + A^T[\mathcal{B}\Upsilon(|\xi) + \overline{\Upsilon}(\xi)], \\ \mathcal{E}(\xi) &= G^T\Upsilon(\xi) + B^T[\mathcal{B}\Upsilon(|\xi) + \overline{\Upsilon}(\xi)], \\ \mathcal{I}(\xi) &= H^T\Upsilon(\xi) + C^T[\mathcal{B}\Upsilon(|\xi) + \overline{\Upsilon}(\xi)], \\ \mathcal{R}(\xi) &= K^T\Upsilon(\xi) + D^T[\mathcal{B}\Upsilon(|\xi) + \overline{\Upsilon}(\xi)], \\ \mathcal{Q}(\xi) &= L^T\Upsilon(\xi) + E^T[\mathcal{B}\Upsilon(|\xi) + \overline{\Upsilon}(\xi)], \end{aligned}\right\} \tag{4.2}$$

where A, B, C, D, E, F, G, H, K, and L are the known vectors. Now, use the definition of the Caputo-fractional derivative to differentiate equation (4.2) with

respect to ξ fractionally. Then, we obtain,

$$\left.\begin{aligned}
&D_{\delta}^{\alpha}(\mathcal{S}(\delta)) = D_{\delta}^{\alpha}(F^T\mathcal{H}(\delta) + A^T[\mathcal{B}\mathcal{H}(\delta) + \overline{\mathcal{H}}(\delta)]),\\
&D_{\delta}^{\alpha}(\mathcal{E}(\delta)) = D_{\delta}^{\alpha}(G^T\mathcal{H}(\delta) + B^T[\mathcal{B}\mathcal{H}(\delta) + \overline{\mathcal{H}}(\delta)]),\\
&D_{\delta}^{\alpha}(\mathcal{I}(\delta)) = D_{\delta}^{\alpha}(H^T\mathcal{H}(\delta) + C^T[\mathcal{B}\mathcal{H}(\delta) + \overline{\mathcal{H}}(\delta)]),\\
&D_{\delta}^{\alpha}(\mathcal{R}(\delta)) = D_{\delta}^{\alpha}(K^T\mathcal{H}(\delta) + D^T[\mathcal{B}\mathcal{H}(\delta) + \overline{\mathcal{H}}(\delta)]),\\
&D_{\delta}^{\alpha}(\mathcal{Q}(\delta)) = D_{\delta}^{\alpha}(L^T\mathcal{H}(\delta) + E^T[\mathcal{B}\mathcal{H}(\delta) + \overline{\mathcal{H}}(\delta)]).
\end{aligned}\right\} \tag{4.3}$$

Substituting (4.2) and (4.3) in (4.1), we get,

$$\left.\begin{aligned}
&D_{\xi}^{\alpha}(F^T\Upsilon(\xi) + A^T\left[\mathcal{B}\Upsilon(\xi) + \bar{\Upsilon}(\xi)\right]) = \theta - \delta F^T\Upsilon(\xi) + A^T[\mathcal{B}\Upsilon(\xi) + \bar{\Upsilon}(\xi)]\\
&(L^T\Upsilon(\xi) + E^T\left[\mathcal{B}\Upsilon(\xi) + \bar{\Upsilon}(\xi)\right]\left(1 + \epsilon(F^T\Upsilon(\xi) + A^T\left[\mathcal{B}\Upsilon(\xi) + \bar{\Upsilon}(\xi)\right]\right)\\
&-\psi\left(F^T\Upsilon(\xi) + A^T\left[\mathcal{B}\Upsilon(\xi) + \bar{\Upsilon}(\xi)\right]\right),\\
&D_{\xi}^{\alpha}(G^T\Upsilon(\xi) + B^T\left[\mathcal{B}\Upsilon(\xi) + \bar{\Upsilon}(\xi)\right]) = \delta\left(F^T\Upsilon(\xi) + A^T\left[\mathcal{B}\Upsilon(\xi) + \bar{\Upsilon}(\xi)\right]\right)\\
&\left(L^T\,\Upsilon(\xi) + E^T\left[\mathcal{B}\Upsilon(\xi) + \bar{\Upsilon}(\xi)\right]\right)\left(1 + \epsilon(F^T\Upsilon(\xi) + A^T\left[\mathcal{B}\Upsilon(\xi) + \bar{\Upsilon}(\xi)\right])\right)\\
&-(\tau + \psi)\left(G^T\Upsilon(\xi) + \,B^T\left[\mathcal{B}\Upsilon(\xi) + \bar{\Upsilon}(\xi)\right]\right),\\
&D_{\xi}^{\alpha}(H^T\Upsilon(\xi) + C^T\left[\mathcal{B}\Upsilon(\xi) + \bar{\Upsilon}(\xi)\right]) = \tau\left(G^T\Upsilon(\xi) + B^T\left[\mathcal{B}\Upsilon(\xi) + \bar{\Upsilon}(\xi)\right]\right)\\
&-\psi\left(H^T\Upsilon(\xi) + C^T\left[\mathcal{B}\Upsilon(\xi) + \bar{\Upsilon}(\xi)\right]\right),\\
&D_{\xi}^{\alpha}(K^T\Upsilon(\xi) + D^T\left[\mathcal{B}\Upsilon(\xi) + \bar{\Upsilon}(\xi)\right]) = \lambda - a\left(H^T\Upsilon(\xi) + C^T\left[\mathcal{B}\Upsilon(\xi) + \bar{\Upsilon}(\xi)\right]\right)\\
&\left(K^T\Upsilon(\xi) + D^T\left[\mathcal{B}\Upsilon(\xi) + \bar{\Upsilon}(\xi)\right]\right)\left(1 + \kappa\left(H^T\Upsilon(\xi) + \,C^T\left[\mathcal{B}\Upsilon(\xi) + \bar{\Upsilon}(\xi)\right]\right)\right)\\
&-\beta\left(K^T\Upsilon(\xi) + D^T\left[\mathcal{B}\Upsilon(\xi) + \bar{\Upsilon}(\xi)\right]\right),\\
&D_{\xi}^{\alpha}(L^T\Upsilon(\xi) + E^T\left[\mathcal{B}\Upsilon(\xi) + \bar{\Upsilon}(\xi)\right]) = a\left(H^T\Upsilon(\xi) + C^T\left[\mathcal{B}\Upsilon(\xi) + \bar{\Upsilon}(\xi)\right]\right)\\
&\left(K^T\Upsilon(\xi) + D^T\left[\mathcal{B}\Upsilon(\xi) + \bar{\Upsilon}(\xi)\right]\right)\left(1 + \kappa\left(H^T\Upsilon(\xi) + C^T\left[\mathcal{B}\Upsilon(\xi) + \bar{\Upsilon}(\xi)\right]\right)\right)\\
&-\beta\left(L^T\Upsilon(\xi) + E^T\left[\mathcal{B}\Upsilon(\xi) + \bar{\Upsilon}(\xi)\right]\right).
\end{aligned}\right\}$$

Collocating the above equations to the subsequent collocation locations $\xi_i = \frac{2i-1}{2^k M}$, $i = 1,\ 2 \dots M$, we obtain,

$$\left.\begin{aligned}
&D^{\alpha}_{\xi}(F^T\Upsilon(\xi_i) + A^T\left[\mathcal{B}\Upsilon\left(\xi_i\right) + \bar{\Upsilon}(\xi_i)\right]) = \theta - \delta F^T\Upsilon\left(\xi_i\right) + A^T[\mathcal{B}\Upsilon\left(\xi_i\right) + \bar{\Upsilon}\left(\xi_i\right)]\\
&(L^T\Upsilon\left(\xi_i\right) + E^T\left[\mathcal{B}\Upsilon\left(\xi_i\right) + \bar{\Upsilon}\left(\xi_i\right)\right]\left(1 + \epsilon(F^T\Upsilon(\xi_i) + A^T\left[\mathcal{B}\Upsilon\left(\xi_i\right) + \bar{\Upsilon}(\xi_i)\right]\right)\\
&-\psi\left(F^T\Upsilon\left(\xi_i\right) + A^T\left[\mathcal{B}\Upsilon\left(\xi_i\right) + \bar{\Upsilon}\left(\xi_i\right)\right]\right),\\
&D^{\alpha}_{\xi}(G^T\Upsilon\left(\xi_i\right) + B^T\left[\mathcal{B}\Upsilon\left(\xi_i\right) + \bar{\Upsilon}\left(\xi_i\right)\right]) = \delta\left(F^T\Upsilon\left(\xi_i\right) + A^T\left[\mathcal{B}\Upsilon\left(\xi_i\right) + \bar{\Upsilon}\left(\xi_i\right)\right]\right)\\
&\left(L^T\ \Upsilon\left(\xi_i\right) + E^T\left[\mathcal{B}\Upsilon\left(\xi_i\right) + \bar{\Upsilon}\left(\xi_i\right)\right]\right)\left(1 + \epsilon(F^T\Upsilon\left(\xi_i\right) + A^T\left[\mathcal{B}\Upsilon\left(\xi_i\right) + \bar{\Upsilon}\left(\xi_i\right)\right])\right)\\
&-(\tau + \psi)\left(G^T\Upsilon\left(\xi_i\right) + \ B^T\left[\mathcal{B}\Upsilon\left(\xi_i\right) + \bar{\Upsilon}\left(\xi_i\right)\right]\right),\\
&D^{\alpha}_{\xi}(H^T\Upsilon\left(\xi_i\right) + C^T\left[\mathcal{B}\Upsilon\left(\xi_i\right) + \bar{\Upsilon}\left(\xi_i\right)\right]) = \tau\left(G^T\Upsilon\left(\xi_i\right) + B^T\left[\mathcal{B}\Upsilon\left(\xi_i\right) + \bar{\Upsilon}\left(\xi_i\right)\right]\right)\\
&-\psi\left(H^T\Upsilon\left(\xi_i\right) + C^T\left[\mathcal{B}\Upsilon\left(\xi_i\right) + \bar{\Upsilon}\left(\xi_i\right)\right]\right),\\
&D^{\alpha}_{\xi}(K^T\Upsilon\left(\xi_i\right) + D^T\left[\mathcal{B}\Upsilon\left(\xi_i\right) + \bar{\Upsilon}\left(\xi_i\right)\right]) = \lambda - a\left(H^T\Upsilon\left(\xi_i\right) + C^T\left[\mathcal{B}\Upsilon\left(\xi_i\right) + \bar{\Upsilon}\left(\xi_i\right)\right]\right)\\
&\left(K^T\Upsilon\left(\xi_i\right) + D^T\left[\mathcal{B}\Upsilon\left(\xi_i\right) + \bar{\Upsilon}\left(\xi_i\right)\right]\right)\left(1 + \kappa\left(H^T\Upsilon\left(\xi_i\right) + \ C^T\left[\mathcal{B}\Upsilon\left(\xi_i\right) + \bar{\Upsilon}\left(\xi_i\right)\right]\right)\right)\\
&-\beta\left(K^T\Upsilon\left(\xi_i\right) + D^T\left[\mathcal{B}\Upsilon\left(\xi_i\right) + \bar{\Upsilon}\left(\xi_i\right)\right]\right),\\
&D^{\alpha}_{\xi}(L^T\Upsilon(\xi_i) + E^T\left[\mathcal{B}\Upsilon\left(\xi_i\right) + \bar{\Upsilon}\left(\xi_i\right)\right]) = a\left(H^T\Upsilon\left(\xi_i\right) + C^T\left[\mathcal{B}\Upsilon\left(\xi_i\right) + \bar{\Upsilon}\left(\xi_i\right)\right]\right)\\
&\left(K^T\Upsilon\left(\xi_i\right) + D^T\left[\mathcal{B}\Upsilon\left(\xi_i\right) + \bar{\Upsilon}\left(\xi_i\right)\right]\right)\left(1 + \kappa\left(H^T\Upsilon\left(\xi_i\right) + C^T\left[\mathcal{B}\Upsilon\left(\xi_i\right) + \bar{\Upsilon}\left(\xi_i\right)\right]\right)\right)\\
&-\beta\left(L^T\Upsilon\left(\xi_i\right) + E^T\left[\mathcal{B}\Upsilon\left(\xi_i\right) + \bar{\Upsilon}\left(\xi_i\right)\right]\right).
\end{aligned}\right\} \tag{4.4}$$

Let

$$f_i\left(\xi_1,\xi_2,\ldots,\xi_i\right)=D_\xi^\alpha(F^T\Upsilon(\xi_i)+A^T\left[\mathcal{B}\Upsilon\left(\xi_i\right)+\bar{\Upsilon}(\xi_i)\right])-\theta+\delta F^T\Upsilon\left(\xi_i\right)+A^T[\mathcal{B}\Upsilon\left(\xi_i\right)$$
$$+\bar{\Upsilon}\left(\xi_i\right)](L^T\Upsilon\left(\xi_i\right)+E^T\left[\mathcal{B}\Upsilon\left(\xi_i\right)+\bar{\Upsilon}\left(\xi_i\right)\right]\left(1+\epsilon(F^T\Upsilon(\xi_i)+A^T\left[\mathcal{B}\Upsilon\left(\xi_i\right)+\bar{\Upsilon}(\xi_i)\right]\right)$$
$$+\psi\left(F^T\Upsilon\left(\xi_i\right)+A^T\left[\mathcal{B}\Upsilon\left(\xi_i\right)+\bar{\Upsilon}\left(\xi_i\right)\right]\right),$$
$$g_i\left(\xi_1,\xi_2,\ldots,\xi_i\right)=D_\xi^\alpha(G^T\Upsilon\left(\xi_i\right)+B^T\left[\mathcal{B}\Upsilon\left(\xi_i\right)+\bar{\Upsilon}\left(\xi_i\right)\right])-\delta(F^T\Upsilon\left(\xi_i\right)+A^T[\mathcal{B}\Upsilon\left(\xi_i\right)$$
$$+\bar{\Upsilon}\left(\xi_i\right)])\left(L^T\ \Upsilon\left(\xi_i\right)+E^T\left[\mathcal{B}\Upsilon\left(\xi_i\right)+\bar{\Upsilon}\left(\xi_i\right)\right]\right)\left(1+\epsilon(F^T\Upsilon\left(\xi_i\right)+A^T\left[\mathcal{B}\Upsilon\left(\xi_i\right)+\bar{\Upsilon}\left(\xi_i\right)\right])\right)$$
$$+(\tau+\psi)\left(G^T\Upsilon\left(\xi_i\right)+\ B^T\left[\mathcal{B}\Upsilon\left(\xi_i\right)+\bar{\Upsilon}\left(\xi_i\right)\right]\right),$$
$$h_i\left(\xi_1,\xi_2,\ldots,\xi_i\right)=D_\xi^\alpha(H^T\Upsilon\left(\xi_i\right)+C^T\left[\mathcal{B}\Upsilon\left(\xi_i\right)+\bar{\Upsilon}\left(\xi_i\right)\right])-\tau(G^T\Upsilon\left(\xi_i\right)+B^T[\mathcal{B}\Upsilon\left(\xi_i\right)$$
$$+\bar{\Upsilon}\left(\xi_i\right)])+\psi\left(H^T\Upsilon\left(\xi_i\right)+C^T\left[\mathcal{B}\Upsilon\left(\xi_i\right)+\bar{\Upsilon}\left(\xi_i\right)\right]\right),$$
$$m_i\left(\xi_1,\xi_2,\ldots,\xi_i\right)=D_\xi^\alpha(K^T\Upsilon\left(\xi_i\right)+D^T\left[\mathcal{B}\Upsilon\left(\xi_i\right)+\bar{\Upsilon}\left(\xi_i\right)\right])-\lambda-a$$
$$(H^T\Upsilon\left(\xi_i\right)+C^T\left[\mathcal{B}\Upsilon\left(\xi_i\right)+\bar{\Upsilon}\left(\xi_i\right)\right])\left(K^T\Upsilon\left(\xi_i\right)+D^T\left[\mathcal{B}\Upsilon\left(\xi_i\right)+\bar{\Upsilon}\left(\xi_i\right)\right]\right)$$
$$\left(1+\kappa\left(H^T\Upsilon\left(\xi_i\right)+\ C^T\left[\mathcal{B}\Upsilon\left(\xi_i\right)+\bar{\Upsilon}\left(\xi_i\right)\right]\right)\right)\beta\left(K^T\Upsilon\left(\xi_i\right)+D^T\left[\mathcal{B}\Upsilon\left(\xi_i\right)+\bar{\Upsilon}\left(\xi_i\right)\right]\right),$$
$$e_i\left(\xi_1,\xi_2,\ldots,\xi_i\right)=D_\xi^\alpha(L^T\Upsilon(\xi_i)+E^T\left[\mathcal{B}\Upsilon\left(\xi_i\right)+\bar{\Upsilon}\left(\xi_i\right)\right])=a(H^T\Upsilon\left(\xi_i\right)$$
$$+C^T\left[\mathcal{B}\Upsilon\left(\xi_i\right)+\bar{\Upsilon}\left(\xi_i\right)\right])\left(K^T\Upsilon\left(\xi_i\right)+D^T\left[\mathcal{B}\Upsilon\left(\xi_i\right)+\bar{\Upsilon}\left(\xi_i\right)\right]\right)$$
$$\left(1+\kappa\left(H^T\Upsilon\left(\xi_i\right)+C^T\left[\mathcal{B}\Upsilon\left(\xi_i\right)+\bar{\Upsilon}\left(\xi_i\right)\right]\right)\right)+\beta\left(L^T\Upsilon\left(\xi_i\right)+E^T\left[\mathcal{B}\Upsilon\left(\xi_i\right)+\bar{\Upsilon}\left(\xi_i\right)\right]\right).$$

If the elements of a single iteration $\xi^{(l)}\in\ \mathbb{R}$ are identified as $\xi_1^{(l)},\xi_2^{(l)},\ldots,\xi_i^{(l)}$, then the equations about these elements are as follows:

$$f_1\left(\xi_1^{(l+1)},\xi_2^{(l+1)},\ldots,\xi_i^{(l+1)}\right)=f\left(\xi_1^{(l)},\xi_2^{(l)},\ldots,\xi_i^{(l)}\right)+\left.\frac{\partial f_1}{\partial\xi_1}\right|_{\xi^{(l)}}\left(\xi_1^{(l+1)}-\xi_1^{(l)}\right)+\left.\frac{\partial f_1}{\partial\xi_2}\right|_{\xi^{(l)}}$$
$$\left(\xi_2^{(l+1)}-\xi_2^{(l)}\right)+\ldots+\left.\frac{\partial f_1}{\partial\xi_i}\right|_{\xi^{(l)}}\left(\xi_i^{(l+1)}-\xi_i^{(l)}\right),$$
$$g_1\left(\xi_1^{(l+1)},\xi_2^{(l+1)},\ldots,\xi_i^{(l+1)}\right)=g\left(\xi!_1^{(l)},\xi_2^{(l)},\ldots,\xi_i^{(l)}\right)+\left.\frac{\partial g_1}{\partial\xi_1}\right|_{\xi^{(l)}}\left(\xi_1^{(l+1)}-\xi_1^{(l)}\right)+\left.\frac{\partial g_1}{\partial\xi_2}\right|_{\xi^{(l)}}$$
$$\left(\xi_2^{(l+1)}-\xi_2^{(l)}\right)+\ldots+\left.\frac{\partial g}{\partial\xi_i}\right|_{\xi^{(l)}}\left(\xi_i^{(l+1)}-\xi_i^{(l)}\right),$$
$$h_1\left(\xi_1^{(l+1)},\xi_2^{(l+1)},\ldots,\xi_i^{(l+1)}\right)=h\left(\xi_1^{(l)},\xi_2^{(l)},\ldots,\xi_i^{(l)}\right)+\left.\frac{\partial h_1}{\partial\xi_1}\right|_{\xi^{(l)}}\left(\xi_1^{(l+1)}-\xi_1^{(l)}\right)+\left.\frac{\partial h_1}{\partial\xi_2}\right|_{\xi^{(l)}}$$
$$\left(\xi_2^{(l+1)}-\xi_2^{(l)}\right)+\ldots+\left.\frac{\partial h}{\partial\xi_i}\right|_{\xi^{(l)}}\left(\xi_i^{(l+1)}-\xi_i^{(l)}\right),$$
$$m_1\left(\xi_1^{(l+1)},\xi_2^{(l+1)},\ldots,\xi_i^{(l+1)}\right)=m\left(\xi_1^{(l)},\xi_2^{(l)},\ldots,\xi_i^{(l)}\right)+\left.\frac{\partial m_1}{\partial\xi_1}\right|_{\xi^{(l)}}\left(\xi_1^{(l+1)}-\xi_1^{(l)}\right)+\left.\frac{\partial m_1}{\partial\xi_2}\right|_{\xi^{(l)}}$$
$$\left(\xi_2^{(l+1)}-\xi_2^{(l)}\right)+\ldots+\left.\frac{\partial m}{\partial\xi_i}\right|_{\xi^{(l)}}\left(\xi_i^{(l+1)}-\xi_i^{(l)}\right),$$
$$e_1\left(\xi_1^{(l+1)},\xi_2^{(l+1)},\ldots,\xi_i^{(l+1)}\right)=e\left(\xi_1^{(l)},\xi_2^{(l)},\ldots,\xi_i^{(l)}\right)+\left.\frac{\partial e_1}{\partial\xi_1}\right|_{\xi^{(l)}}\left(\xi_1^{(l+1)}-\xi_1^{(l)}\right)+\left.\frac{\partial e_1}{\partial\xi_2}\right|_{\xi^{(l)}}$$
$$\left(\xi_2^{(l+1)}-\xi_2^{(l)}\right)+\ldots+\left.\frac{\partial m}{\partial\xi_i}\right|_{\xi^{(l)}}\left(\xi_i^{(l+1)}-\xi_i^{(l)}\right).$$

Making use of the Taylor expansion for the functions $f_2, f_3, \ldots, f_i, g_2, g_3, \ldots, g_i$, $h_2, h_3, \ldots, h_i, m_2, m_3, \ldots, m_i$, and $e_2, e_3, \ldots, e_i$, in a similar way,

$$\begin{pmatrix} f_1\left(\xi^{(l+1)}\right) \\ f_2\left(\xi^{(l+1)}\right) \\ \vdots \\ f_i\left(\xi^{(l+1)}\right) \end{pmatrix} = \begin{pmatrix} f_1\left(\xi^{(i)}\right) \\ f_2\left(\xi^{(i)}\right) \\ \vdots \\ f_i\left(\xi^{(i)}\right) \end{pmatrix} + \begin{pmatrix} \frac{\partial f_1}{\partial \xi_1}\Big|_{\xi^{(l)}} & \frac{\partial f_1}{\partial \xi_2}\Big|_{\xi^{(l)}} & \cdots & \frac{\partial f_1}{\partial \xi_i}\Big|_{\xi^{(l)}} \\ \frac{\partial f_2}{\partial \xi_1}\Big|_{\xi^{(l)}} & \frac{\partial f_2}{\partial \xi_2}\Big|_{\xi^{(l)}} & \cdots & \frac{\partial f_2}{\partial \xi_i}\Big|_{\xi^{(l)}} \\ \vdots & \vdots & & \vdots \\ \frac{\partial f_i}{\partial \xi_1}\Big|_{\xi^{(l)}} & \frac{\partial f_i}{\partial \xi_2}\Big|_{\xi^{(l)}} & \cdots & \frac{\partial f_i}{\partial \xi_i}\Big|_{\xi^{(l)}} \end{pmatrix} \begin{pmatrix} \left(\xi_1^{(l+1)} - \xi_1^{(l)}\right) \\ \left(\xi_2^{(l+1)} - \xi_2^{(l)}\right) \\ \vdots \\ \left(\xi_i^{(l+1)} - \xi_i^{(l)}\right) \end{pmatrix},$$

$$\begin{pmatrix} g_1\left(\xi^{(l+1)}\right) \\ g_2\left(\xi^{(l+1)}\right) \\ \vdots \\ g_i\left(\xi^{(l+1)}\right) \end{pmatrix} = \begin{pmatrix} g_1\left(\xi^{(i)}\right) \\ g_2\left(\xi^{(i)}\right) \\ \vdots \\ g_i\left(\xi^{(i)}\right) \end{pmatrix} + \begin{pmatrix} \frac{\partial g_1}{\partial \xi_1}\Big|_{\xi^{(l)}} & \frac{\partial g_1}{\partial \xi_2}\Big|_{\xi^{(l)}} & \cdots & \frac{\partial g_1}{\partial \xi_i}\Big|_{\xi^{(l)}} \\ \frac{\partial g_2}{\partial \xi_1}\Big|_{\xi^{(l)}} & \frac{\partial g_2}{\partial \xi_2}\Big|_{\xi^{(l)}} & \cdots & \frac{\partial g_2}{\partial \xi_i}\Big|_{\xi^{(l)}} \\ \vdots & \vdots & & \vdots \\ \frac{\partial g_i}{\partial \xi_1}\Big|_{\xi^{(l)}} & \frac{\partial g_i}{\partial \xi_2}\Big|_{\xi^{(l)}} & \cdots & \frac{\partial g_i}{\partial \xi_i}\Big|_{\xi^{(l)}} \end{pmatrix} \begin{pmatrix} \left(\xi_1^{(l+1)} - \xi_1^{(l)}\right) \\ \left(\xi_2^{(l+1)} - \xi_2^{(l)}\right) \\ \vdots \\ \left(\xi_i^{(l+1)} - \xi_i^{(l)}\right) \end{pmatrix},$$

$$\begin{pmatrix} h_1\left(\xi^{(l+1)}\right) \\ h_2\left(\xi^{(l+1)}\right) \\ \vdots \\ h_i\left(\xi^{(l+1)}\right) \end{pmatrix} = \begin{pmatrix} h_1\left(\xi^{(i)}\right) \\ h_2\left(\xi^{(i)}\right) \\ \vdots \\ h_i\left(\xi^{(i)}\right) \end{pmatrix} + \begin{pmatrix} \frac{\partial h_1}{\partial \xi_1}\Big|_{\xi^{(l)}} & \frac{\partial h_1}{\partial \xi_2}\Big|_{\xi^{(l)}} & \cdots & \frac{\partial h_1}{\partial \xi_i}\Big|_{\xi^{(l)}} \\ \frac{\partial h_2}{\partial \xi_1}\Big|_{\xi^{(l)}} & \frac{\partial h_2}{\partial \xi_2}\Big|_{\xi^{(l)}} & \cdots & \frac{\partial h_2}{\partial \xi_i}\Big|_{\xi^{(l)}} \\ \vdots & \vdots & & \vdots \\ \frac{\partial h_i}{\partial \xi_1}\Big|_{\xi^{(l)}} & \frac{\partial h_i}{\partial \xi_2}\Big|_{\xi^{(l)}} & \cdots & \frac{\partial h_i}{\partial \xi_i}\Big|_{\xi^{(l)}} \end{pmatrix} \begin{pmatrix} \left(\xi_1^{(l+1)} - \xi_1^{(l)}\right) \\ \left(\xi_2^{(l+1)} - \xi_2^{(l)}\right) \\ \vdots \\ \left(\xi_i^{(l+1)} - \xi_i^{(l)}\right) \end{pmatrix},$$

$$\begin{pmatrix} m_1\left(\xi^{(l+1)}\right) \\ m_2\left(\xi^{(l+1)}\right) \\ \vdots \\ m_i\left(\xi^{(l+1)}\right) \end{pmatrix} = \begin{pmatrix} m_1\left(\xi^{(i)}\right) \\ m_2\left(\xi^{(i)}\right) \\ \vdots \\ m_i\left(\xi^{(i)}\right) \end{pmatrix} + \begin{pmatrix} \frac{\partial m_1}{\partial \xi_1}\Big|_{\xi^{(l)}} & \frac{\partial m_1}{\partial \xi_2}\Big|_{\xi^{(l)}} & \cdots & \frac{\partial m_1}{\partial \xi_i}\Big|_{\xi^{(l)}} \\ \frac{\partial m_2}{\partial \xi_1}\Big|_{\xi^{(l)}} & \frac{\partial m_2}{\partial \xi_2}\Big|_{\xi^{(l)}} & \cdots & \frac{\partial m_2}{\partial \xi_i}\Big|_{\xi^{(l)}} \\ \vdots & \vdots & & \vdots \\ \frac{\partial m_i}{\partial \xi_1}\Big|_{\xi^{(l)}} & \frac{\partial m_i}{\partial \xi_2}\Big|_{\xi^{(l)}} & \cdots & \frac{\partial m_i}{\partial \xi_i}\Big|_{\xi^{(l)}} \end{pmatrix} \begin{pmatrix} \left(\xi_1^{(l+1)} - \xi_1^{(l)}\right) \\ \left(\xi_2^{(l+1)} - \xi_2^{(l)}\right) \\ \vdots \\ \left(\xi_i^{(l+1)} - \xi_i^{(l)}\right) \end{pmatrix},$$

$$\begin{pmatrix} e_1\left(\xi^{(l+1)}\right) \\ e_2\left(\xi^{(l+1)}\right) \\ \vdots \\ e_i\left(\xi^{(l+1)}\right) \end{pmatrix} = \begin{pmatrix} e_1\left(\xi^{(i)}\right) \\ e_2\left(\xi^{(i)}\right) \\ \vdots \\ e_i\left(\xi^{(i)}\right) \end{pmatrix} + \begin{pmatrix} \frac{\partial e_1}{\partial \xi_1}\Big|_{\xi^{(l)}} & \frac{\partial e_1}{\partial \xi_2}\Big|_{\xi^{(l)}} & \cdots & \frac{\partial e_1}{\partial \xi_i}\Big|_{\xi^{(l)}} \\ \frac{\partial e_2}{\partial \xi_1}\Big|_{\xi^{(l)}} & \frac{\partial e_2}{\partial \xi_2}\Big|_{\xi^{(l)}} & \cdots & \frac{\partial e_2}{\partial \xi_i}\Big|_{\xi^{(l)}} \\ \vdots & \vdots & & \vdots \\ \frac{\partial e_i}{\partial \xi_1}\Big|_{\xi^{(l)}} & \frac{\partial e_i}{\partial \xi_2}\Big|_{\xi^{(l)}} & \cdots & \frac{\partial e_i}{\partial \xi_i}\Big|_{\xi^{(l)}} \end{pmatrix} \begin{pmatrix} \left(\xi_1^{(l+1)} - \xi_1^{(l)}\right) \\ \left(\xi_2^{(l+1)} - \xi_2^{(l)}\right) \\ \vdots \\ \left(\xi_i^{(l+1)} - \xi_i^{(l)}\right) \end{pmatrix}.$$

Assigning the left side matrix as zero, we obtain,

$$\begin{pmatrix} \frac{\partial f_1}{\partial \xi_1}\Big|_{\xi^{(l)}} & \frac{\partial f_1}{\partial \xi_2}\Big|_{\xi^{(l)}} & \cdots & \frac{\partial f_1}{\partial \xi_i}\Big|_{\xi^{(l)}} \\ \frac{\partial f_2}{\partial \xi_1}\Big|_{\xi^{(l)}} & \frac{\partial f_2}{\partial \xi_2}\Big|_{\xi^{(l)}} & \cdots & \frac{\partial f_2}{\partial \xi_i}\Big|_{\xi^{(l)}} \\ \vdots & \vdots & & \vdots \\ \frac{\partial f_i}{\partial \xi_1}\Big|_{\xi^{(l)}} & \frac{\partial f_i}{\partial \xi_2}\Big|_{\xi^{(l)}} & \cdots & \frac{\partial f_i}{\partial \xi_i}\Big|_{\xi^{(l)}} \end{pmatrix} \begin{pmatrix} \left(\xi_1^{(l+1)} - \xi_1^{(l)}\right) \\ \left(\xi_2^{(l+1)} - \xi_2^{(l)}\right) \\ \vdots \\ \left(\xi_i^{(l+1)} - \xi_i^{(l)}\right) \end{pmatrix} = - \begin{pmatrix} f_1\left(\xi^{(i)}\right) \\ f_2\left(\xi^{(i)}\right) \\ \vdots \\ f_i\left(\xi^{(i)}\right) \end{pmatrix}, \qquad (4.5)$$

$$\begin{pmatrix} \frac{\partial g_1}{\partial \xi_1}\Big|_{\xi^{(l)}} & \frac{\partial g_1}{\partial \xi_2}\Big|_{\xi^{(l)}} & \cdots & \frac{\partial g_1}{\partial \xi_i}\Big|_{\xi^{(l)}} \\ \frac{\partial g_2}{\partial \xi_1}\Big|_{\xi^{(l)}} & \frac{\partial g_2}{\partial \xi_2}\Big|_{\xi^{(l)}} & \cdots & \frac{\partial g_2}{\partial \xi_i}\Big|_{\xi^{(l)}} \\ \vdots & \vdots & & \vdots \\ \frac{\partial g_i}{\partial \xi_1}\Big|_{\xi^{(l)}} & \frac{\partial g_i}{\partial \xi_2}\Big|_{\xi^{(l)}} & \cdots & \frac{\partial g_i}{\partial \xi_i}\Big|_{\xi^{(l)}} \end{pmatrix} \begin{pmatrix} \left(\xi_1^{(l+1)} - \xi_1^{(l)}\right) \\ \left(\xi_2^{(l+1)} - \xi_2^{(l)}\right) \\ \vdots \\ \left(\xi_i^{(l+1)} - \xi_i^{(l)}\right) \end{pmatrix} = - \begin{pmatrix} g_1\left(\xi^{(i)}\right) \\ g_2\left(\xi^{(i)}\right) \\ \vdots \\ g_i\left(\xi^{(i)}\right) \end{pmatrix}, \tag{4.6}$$

$$\begin{pmatrix} \frac{\partial h_1}{\partial \xi_1}\Big|_{\xi^{(l)}} & \frac{\partial h_1}{\partial \xi_2}\Big|_{\xi^{(l)}} & \cdots & \frac{\partial h_1}{\partial \xi_i}\Big|_{\xi^{(l)}} \\ \frac{\partial h_2}{\partial \xi_1}\Big|_{\xi^{(l)}} & \frac{\partial h_2}{\partial \xi_2}\Big|_{\xi^{(l)}} & \cdots & \frac{\partial h_2}{\partial \xi_i}\Big|_{\xi^{(l)}} \\ \vdots & \vdots & & \vdots \\ \frac{\partial h_i}{\partial \xi_1}\Big|_{\xi^{(l)}} & \frac{\partial h_i}{\partial \xi_2}\Big|_{\xi^{(l)}} & \cdots & \frac{\partial h_i}{\partial \xi_i}\Big|_{\xi^{(l)}} \end{pmatrix} \begin{pmatrix} \left(\xi_1^{(l+1)} - \xi_1^{(l)}\right) \\ \left(\xi_2^{(l+1)} - \xi_2^{(l)}\right) \\ \vdots \\ \left(\xi_i^{(l+1)} - \xi_i^{(l)}\right) \end{pmatrix} = - \begin{pmatrix} h_1\left(\xi^{(i)}\right) \\ h_2\left(\xi^{(i)}\right) \\ \vdots \\ h_i\left(\xi^{(i)}\right) \end{pmatrix}, \tag{4.7}$$

$$\begin{pmatrix} \frac{\partial m_1}{\partial \xi_1}\Big|_{\xi^{(l)}} & \frac{\partial m_1}{\partial \xi_2}\Big|_{\xi^{(l)}} & \cdots & \frac{\partial m_1}{\partial \xi_i}\Big|_{\xi^{(l)}} \\ \frac{\partial m_2}{\partial \xi_1}\Big|_{\xi^{(l)}} & \frac{\partial m_2}{\partial \xi_2}\Big|_{\xi^{(l)}} & \cdots & \frac{\partial m_2}{\partial \xi_i}\Big|_{\xi^{(l)}} \\ \vdots & \vdots & & \vdots \\ \frac{\partial m_i}{\partial \xi_1}\Big|_{\xi^{(l)}} & \frac{\partial m_i}{\partial \xi_2}\Big|_{\xi^{(l)}} & \cdots & \frac{\partial m_i}{\partial \xi_i}\Big|_{\xi^{(l)}} \end{pmatrix} \begin{pmatrix} \left(\xi_1^{(l+1)} - \xi_1^{(l)}\right) \\ \left(\xi_2^{(l+1)} - \xi_2^{(l)}\right) \\ \vdots \\ \left(\xi_i^{(l+1)} - \xi_i^{(l)}\right) \end{pmatrix} = - \begin{pmatrix} m_1\left(\xi^{(i)}\right) \\ m_2\left(\xi^{(i)}\right) \\ \vdots \\ m_i\left(\xi^{(i)}\right) \end{pmatrix}, \tag{4.8}$$

$$\begin{pmatrix} \frac{\partial e_1}{\partial \xi_1}\Big|_{\xi^{(l)}} & \frac{\partial e_1}{\partial \xi_2}\Big|_{\xi^{(l)}} & \cdots & \frac{\partial e_1}{\partial \xi_i}\Big|_{\xi^{(l)}} \\ \frac{\partial e_2}{\partial \xi_1}\Big|_{\xi^{(l)}} & \frac{\partial e_2}{\partial \xi_2}\Big|_{\xi^{(l)}} & \cdots & \frac{\partial e_2}{\partial \xi_i}\Big|_{\xi^{(l)}} \\ \vdots & \vdots & & \vdots \\ \frac{\partial e_i}{\partial \xi_1}\Big|_{\xi^{(l)}} & \frac{\partial e_i}{\partial \xi_2}\Big|_{\xi^{(l)}} & \cdots & \frac{\partial e_i}{\partial \xi_i}\Big|_{\xi^{(l)}} \end{pmatrix} \begin{pmatrix} \left(\xi_1^{(l+1)} - \xi_1^{(l)}\right) \\ \left(\xi_2^{(l+1)} - \xi_2^{(l)}\right) \\ \vdots \\ \left(\xi_i^{(l+1)} - \xi_i^{(l)}\right) \end{pmatrix} = - \begin{pmatrix} e_1\left(\xi^{(i)}\right) \\ e_2\left(\xi^{(i)}\right) \\ \vdots \\ e_i\left(\xi^{(i)}\right) \end{pmatrix}. \tag{4.9}$$

Set $K = \frac{\partial f_i}{\partial \xi_j}\Big|_{\xi^{(l)}}, J = \frac{\partial g_i}{\partial \xi_j}\Big|_{\xi^{(l)}}, W = \frac{\partial h_i}{\partial \xi_j}\Big|_{\xi^{(l)}}$, $V = \frac{\partial m_i}{\partial \xi_j}\Big|_{\xi^{(l)}}$ and $Z = \frac{\partial e_i}{\partial \xi_j}\Big|_{\xi^{(l)}}$ where $K,\ J,\ W,\ V$, and Z are the Jacobian matrices for the systems. Then, we have,

$$\left.\begin{aligned} K\ \Delta x &= -f, \\ J\ \Delta x &= -g, \\ W\ \Delta x &= -h, \\ V\ \Delta x &= -m, \\ Z\ \Delta x &= -e. \end{aligned}\right\}$$

Here, Δx is an $n-$dimensional vector whose components are $\left(\xi_1^{(l+1)} - xi_1^{(l)}\right)$, $\left(\xi_2^{(l+1)} - \xi_2^{(l)}\right)$ and $\left(\xi_i^{(l+1)} - \xi_i^{(l)}\right), K,\ J,\ W,\ V$, and Z are $i \times i$ matrix, $-f, -g, -h$, $-m$ and $-e$ are the vector of n components. Adding the equation mentioned above systems together, we attain $Q\ \Delta x = -p$, where $Q = K + J + W + V + Z$ and $p = f + g + h + m + e$. The system mentioned above can be solved in the following way since Q is invertible:

$$\Delta x = -\frac{Q^{-1}}{p} \quad \Rightarrow \quad \xi^{(l+1)} = \xi^{(l)} - K^{-1}p.$$

The equations mentioned above yield the unidentified Taylor wavelet coefficient values. By replacing these coefficient values in (4.2), one can derive the TWCM numerical solution for the problem.

5. Applications of the projected approach

In general, today's problems are not determinable but have stochastic influence, which offers an additional logical way to illustrate viral dynamics. Here, we employed the TWCM to solve SFODEs. Here, we used the TWCM and the operational matrix from Section 2 to transform the nonlinear differential equations into a set of algebraic equations. Later, with the Newton-Raphson approach, the set of nonlinear algebraic equations is resolved, and the Taylor wavelet coefficients and wavelet-based numerical solutions of $S(\xi)$, $E(\xi)$, $I(\xi)$, $R(\xi)$ and $R(\xi)$ are obtained for the model by substituting these coefficient values. The TWCM solutions produced for the value of $\alpha = 1$ (integer order) are displayed in Tables 6-10. The numerical approximations generated by the created methodology (TWCM) and other current methods are contrasted with the NDSolve solution because no exact solution is available. The findings indicate that, compared to existing methods like the Homotopy analysis transform method (HATM) and RK4 method, the TWCM solutions are closer to the NDSolve results. The results are tabulated in Tables 6-10, and the absolute errors of the developed approach with the NDSolve solution are presented in Tables 1-5. The numerical solutions of the desired model at diverse values of α are computed and listed in Tables 11-15. The pictorial illustrations of the solution at $\alpha = 0.2,\ 0.4,\ 0.6,\ 0.8$, and 1.0, respectively, are drawn in Figures 11-15. Different values of M and k are used to calculate the TWCM solutions. Additionally, as shown in Tables 1-5, we can increase the precision of the results by extending the estimates of M and k. It demonstrates that raising M and k can lead to higher precision. From the numerical data in Figures 1-5, it is evident that when the populations of susceptible pine trees and susceptible insects decrease, the populations of infected pine trees and exposed classes increase. Also, the population of infected beetle classes rises. Additionally, multiple observations of the corresponding decay and growth can be made on various fractional orders. The quantity of susceptible pine trees and beetles reduces when the order α of the fractional derivative is decreased. However, the number of exposed, infected pine trees and beetles dramatically increases, as shown in Figures 11-15. Therefore, based on the graphical data, we may conclude that the model significantly stands on the order of fractional derivatives, which produces biologically realistic outcomes. Additionally, we conclude that, compared to the integer order PWD model, the suggested model under Caputo fractional order derivative offers more prosperous and more flexible outcomes.

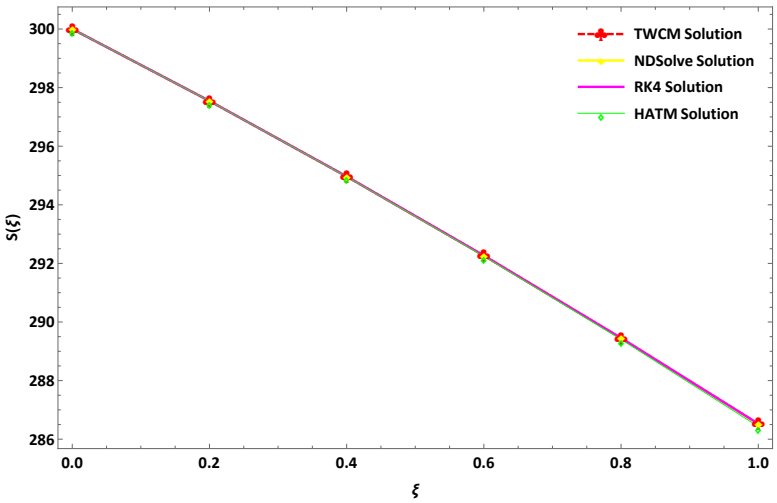

Figure 1. Plot of the Susceptible Pine tree class $S(\xi)$ compared with different methods.

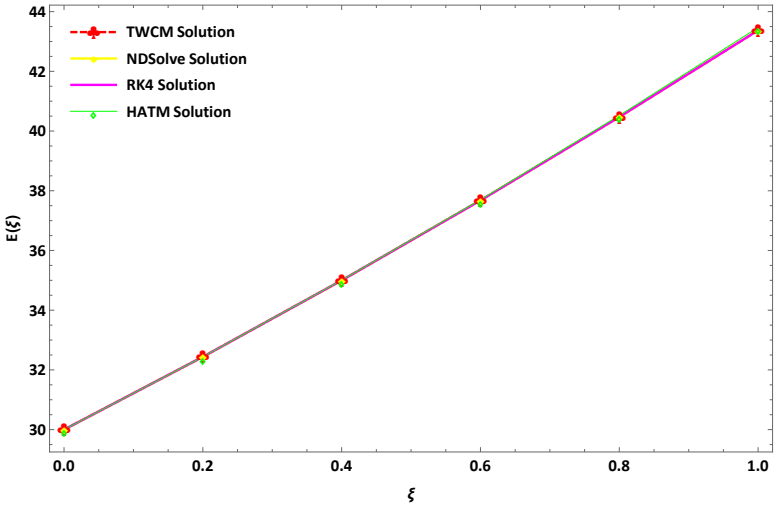

Figure 2. Plot of the Exposed Pine tree class $E(\xi)$ compared with different methods.

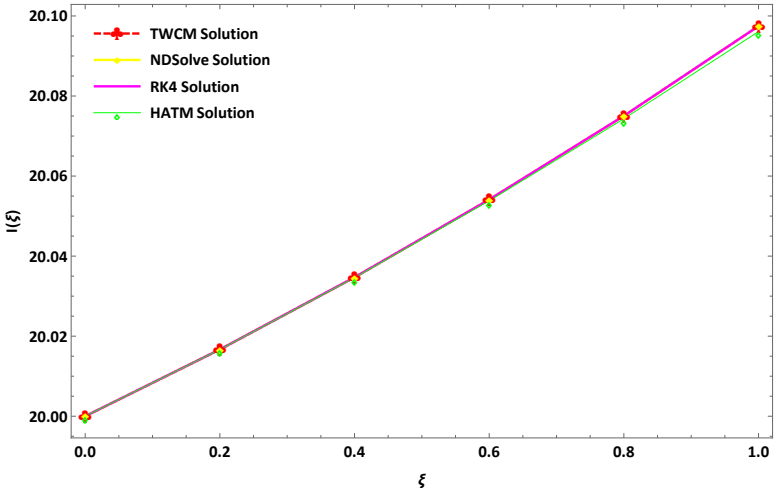

Figure 3. Plot of the Infected Pine tree class $I(\xi)$ compared with different methods.

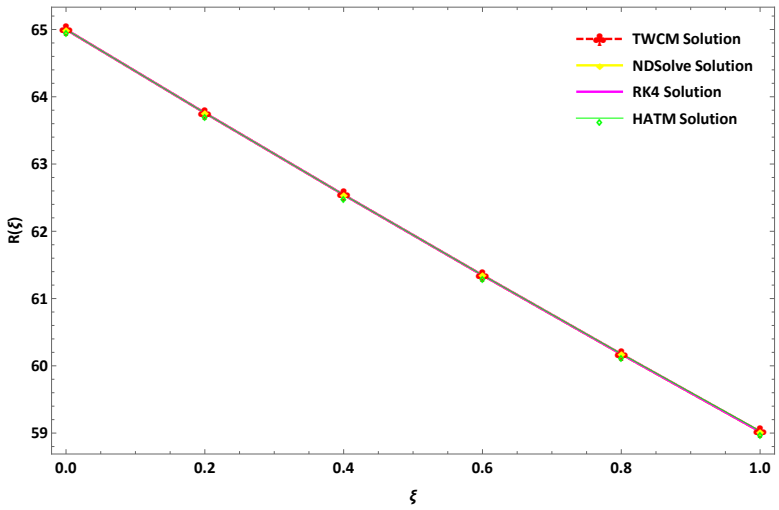

Figure 4. Plot of the Susceptible beetles' class $R(\xi)$ compared with different methods.

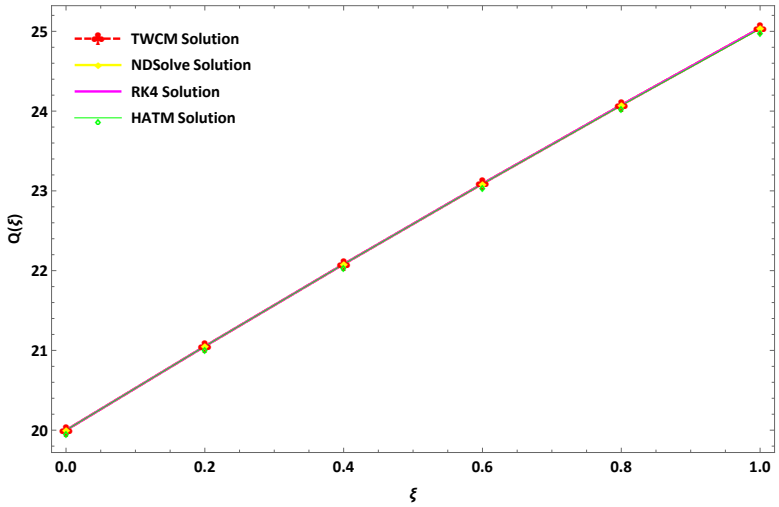

Figure 5. Plot of the Infected beetles' class $Q(\xi)$ compared with different methods.

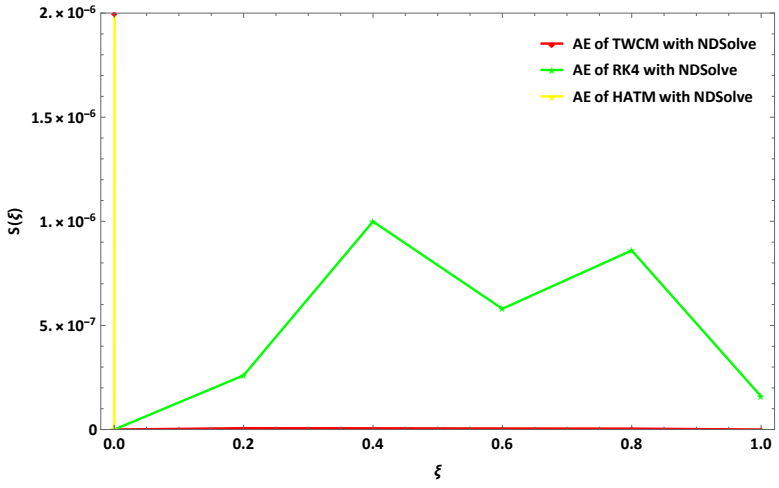

Figure 6. Graphical contrast of AE of $S(\xi)$.

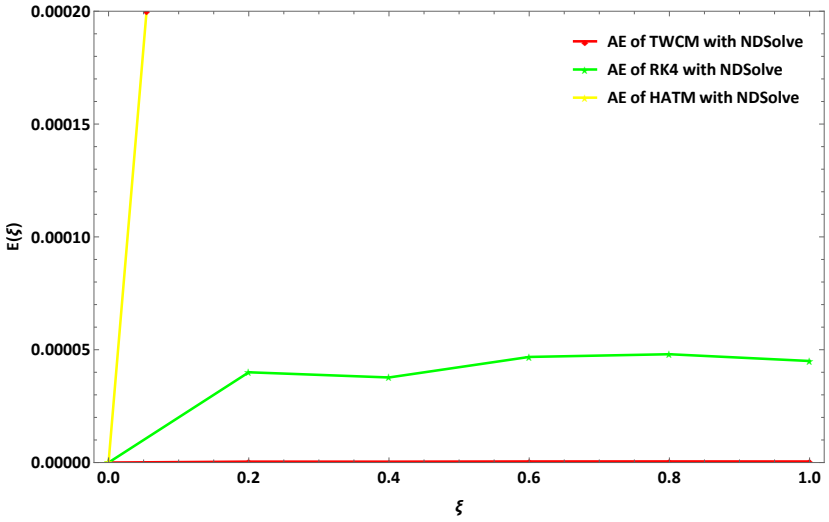

Figure 7. Graphical contrast of AE of $E(\xi)$.

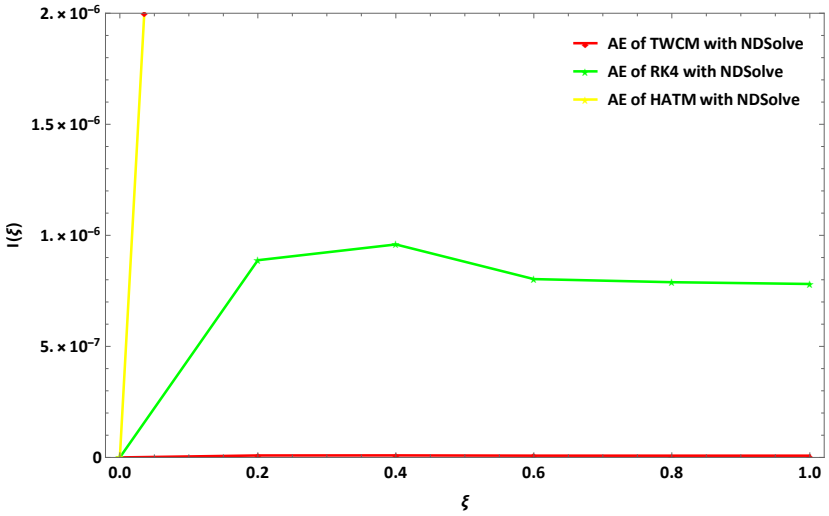

Figure 8. Graphical contrast of AE of $I(\xi)$.

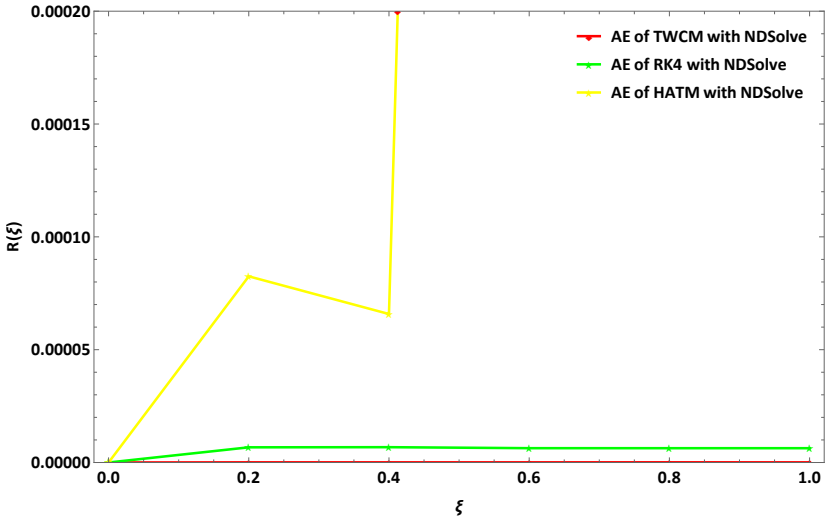

Figure 9. Graphical contrast of AE of $R(\xi)$.

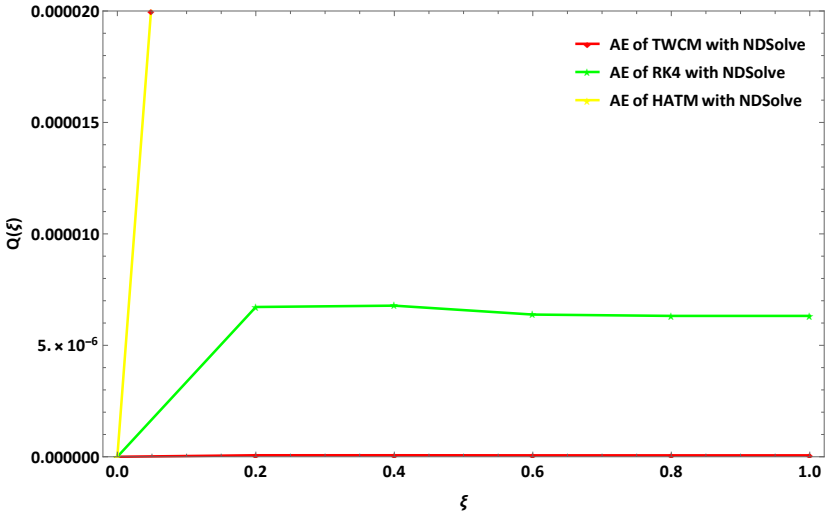

Figure 10. Graphical contrast of AE of $Q(\xi)$.

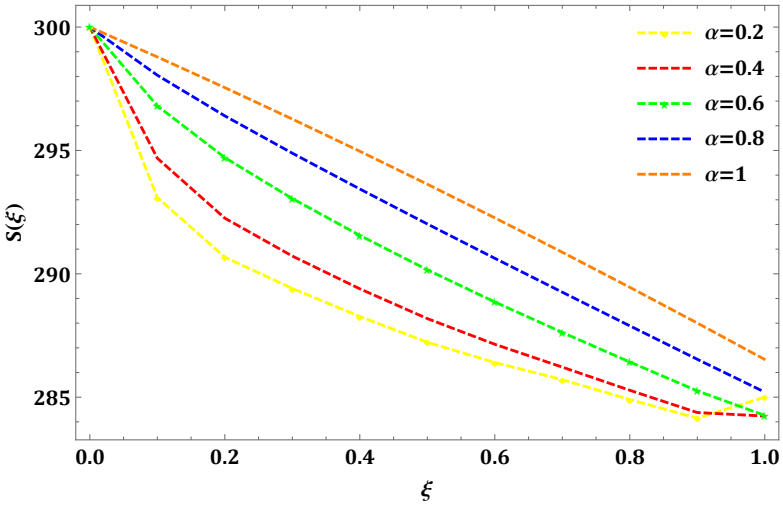

Figure 11. Graphical depiction of $S(\xi)$ with distinct values of α.

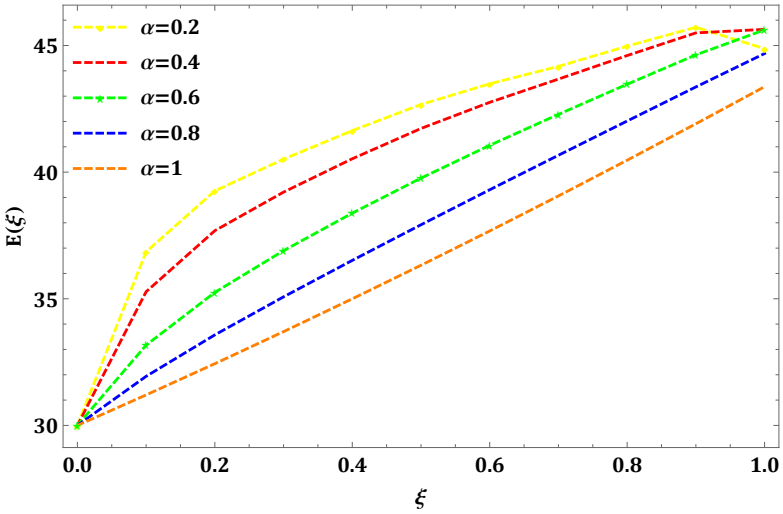

Figure 12. Graphical depiction of $E(\xi)$ with distinct values of α.

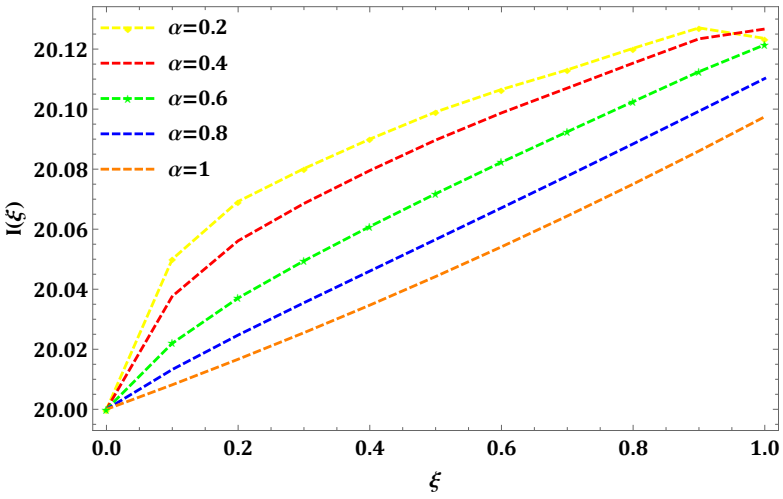

Figure 13. Graphical depiction of $I(\xi)$ with distinct values of α.

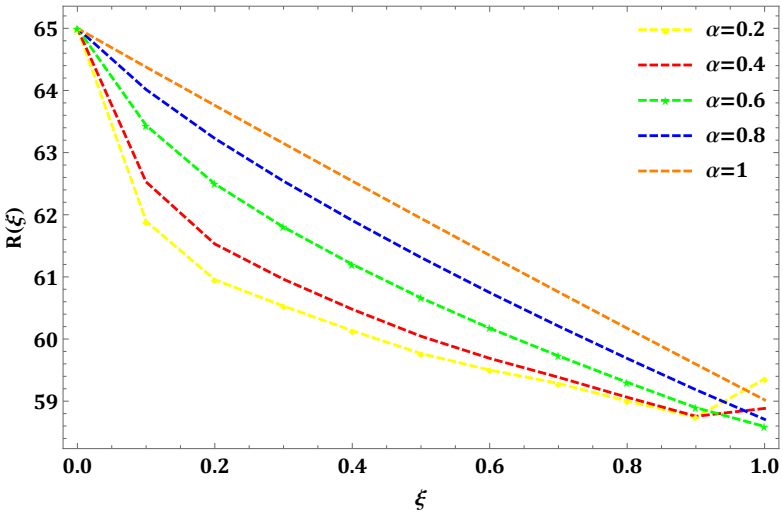

Figure 14. Graphical depiction of $R(\xi)$ with distinct values of α.

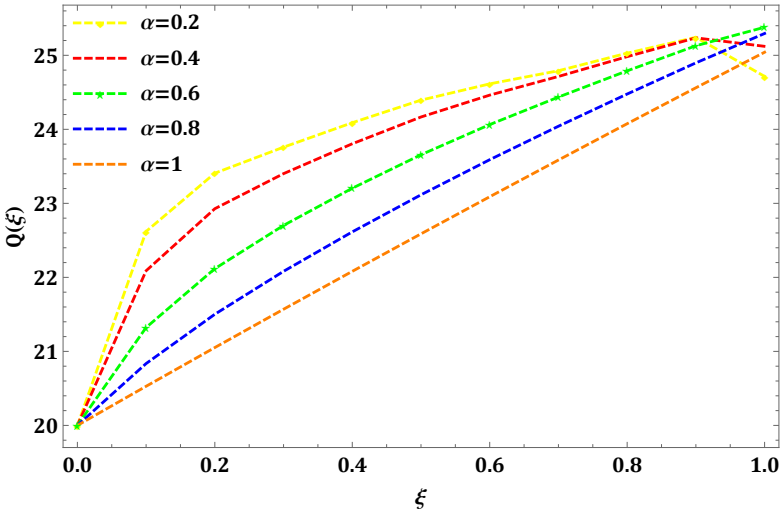

Figure 15. Graphical depiction of $Q(\xi)$ with distinct values of α.

Table 1. **AE assessment of $S(\xi)$ with the several estimates of M and k.**

ξ	**Absolute error of GWCM with NDSolve method**					
	k=1,M=3	**k=2,M=3**	**k=1,M=4**	**k=2,M=4**	**k=1,M=6**	**k=2,M=6**
0	0	0	0	0	0	0
0.1	7.48×10^{-5}	5.82×10^{-6}	3.34×10^{-6}	9.96×10^{-8}	5.50×10^{-9}	6.53×10^{-9}
0.2	8.32×10^{-5}	2.85×10^{-6}	2.93×10^{-6}	6.23×10^{-8}	5.44×10^{-9}	6.18×10^{-9}
0.3	6.35×10^{-5}	2.84×10^{-6}	1.98×10^{-6}	9.04×10^{-8}	5.12×10^{-9}	5.84×10^{-9}
0.4	4.16×10^{-5}	5.73×10^{-6}	1.75×10^{-6}	5.31×10^{-8}	4.69×10^{-9}	5.49×10^{-9}
0.5	3.28×10^{-5}	4.39×10^{-6}	2.20×10^{-6}	4.39×10^{-9}	4.39×10^{-9}	5.15×10^{-9}
0.6	4.14×10^{-5}	4.24×10^{-6}	2.64×10^{-6}	9.41×10^{-8}	4.09×10^{-9}	4.81×10^{-9}
0.7	6.21×10^{-5}	2.09×10^{-6}	2.40×10^{-6}	5.80×10^{-8}	3.67×10^{-9}	4.47×10^{-9}
0.8	8.02×10^{-5}	2.09×10^{-6}	1.46×10^{-6}	8.52×10^{-8}	3.36×10^{-9}	4.13×10^{-9}
0.9	7.26×10^{-5}	4.16×10^{-6}	1.06×10^{-6}	4.91×10^{-8}	3.31×10^{-9}	3.80×10^{-9}
1.0	8.15×10^{-6}	2.64×10^{-7}	4.38×10^{-6}	1.35×10^{-7}	1.48×10^{-9}	1.04×10^{-11}

Table 2. **AE assessment of $E(\xi)$ with the several estimates of M and k.**

ξ	**Absolute error of GWCM with NDSolve method**					
	k=1,M=3	**k=2,M=3**	**k=1,M=4**	**k=2,M=4**	**k=1,M=6**	**k=2,M=6**
0	0	0	0	0	0	0
0.1	7.40×10^{-5}	6.13×10^{-6}	3.73×10^{-6}	4.84×10^{-7}	3.90×10^{-7}	3.91×10^{-7}
0.2	8.23×10^{-5}	3.21×10^{-6}	3.34×10^{-6}	4.60×10^{-7}	4.03×10^{-7}	4.04×10^{-7}
0.3	6.28×10^{-5}	3.14×10^{-6}	2.33×10^{-6}	4.34×10^{-7}	3.48×10^{-7}	3.49×10^{-7}
0.4	4.13×10^{-5}	6.02×10^{-6}	2.14×10^{-6}	4.32×10^{-7}	3.83×10^{-7}	3.84×10^{-7}
0.5	3.27×10^{-5}	4.67×10^{-6}	2.67×10^{-6}	4.67×10^{-7}	4.67×10^{-7}	4.68×10^{-7}
0.6	4.11×10^{-5}	4.63×10^{-6}	3.12×10^{-6}	5.67×10^{-7}	4.77×10^{-7}	4.78×10^{-7}
0.7	6.15×10^{-5}	2.53×10^{-6}	2.89×10^{-6}	5.41×10^{-7}	4.86×10^{-7}	4.87×10^{-7}
0.8	7.93×10^{-5}	2.53×10^{-6}	1.95×10^{-6}	5.57×10^{-7}	4.93×10^{-7}	4.93×10^{-7}
0.9	7.18×10^{-5}	4.54×10^{-6}	1.53×10^{-6}	5.21×10^{-7}	4.75×10^{-7}	4.76×10^{-7}
1.0	8.47×10^{-6}	7.27×10^{-7}	4.86×10^{-6}	6.02×10^{-7}	4.65×10^{-7}	4.67×10^{-7}

Table 3. **AE assessment of $I(\xi)$ with the several estimates of M and k.**

ξ	**Absolute error of GWCM with NDSolve method**					
	k=1,M=3	**k=2,M=3**	**k=1,M=4**	**k=2,M=4**	**k=1,M=6**	**k=2,M=6**
0	0	0	0	0	0	0
0.1	1.14×10^{-6}	7.11×10^{-8}	1.93×10^{-8}	6.79×10^{-9}	6.38×10^{-9}	6.38×10^{-9}
0.2	1.30×10^{-6}	3.01×10^{-8}	1.94×10^{-8}	9.15×10^{-9}	8.92×10^{-9}	8.92×10^{-9}
0.3	1.00×10^{-6}	3.02×10^{-8}	1.55×10^{-8}	9.83×10^{-9}	9.49×10^{-9}	9.49×10^{-9}
0.4	6.71×10^{-7}	7.13×10^{-8}	1.38×10^{-8}	9.29×10^{-9}	9.14×10^{-9}	9.14×10^{-9}
0.5	5.38×10^{-7}	8.12×10^{-9}	1.41×10^{-8}	8.12×10^{-9}	8.12×10^{-9}	8.12×10^{-9}
0.6	6.91×10^{-7}	7.55×10^{-8}	1.52×10^{-8}	8.35×10^{-9}	8.06×10^{-9}	8.06×10^{-9}
0.7	1.05×10^{-6}	3.35×10^{-8}	1.35×10^{-8}	8.15×10^{-9}	8.00×10^{-9}	8.00×10^{-9}
0.8	1.38×10^{-6}	3.40×10^{-8}	9.18×10^{-9}	8.14×10^{-9}	7.92×10^{-9}	7.92×10^{-9}
0.9	1.27×10^{-6}	7.78×10^{-8}	7.31×10^{-9}	8.02×10^{-9}	7.93×10^{-9}	7.93×10^{-9}
1.0	1.44×10^{-7}	4.00×10^{-9}	2.02×10^{-8}	8.24×10^{-9}	7.86×10^{-9}	7.86×10^{-9}

Table 4. **AE assessment of $R(\xi)$ with the several estimates of M and k.**

ξ	**Absolute error of GWCM with NDSolve method**					
	k=1,M=3	**k=2,M=3**	**k=1,M=4**	**k=2,M=4**	**k=1,M=6**	**k=2,M=6**
0	0	0	0	0	0	0
0.1	3.94×10^{-6}	2.21×10^{-7}	7.87×10^{-8}	5.30×10^{-8}	5.21×10^{-8}	5.21×10^{-8}
0.2	4.39×10^{-6}	6.39×10^{-8}	9.11×10^{-8}	6.79×10^{-8}	6.74×10^{-8}	6.74×10^{-8}
0.3	3.30×10^{-6}	6.20×10^{-8}	8.61×10^{-8}	7.02×10^{-8}	6.94×10^{-8}	6.94×10^{-8}
0.4	2.07×10^{-7}	2.06×10^{-7}	8.30×10^{-8}	6.85×10^{-8}	6.80×10^{-8}	6.80×10^{-8}
0.5	1.57×10^{-7}	6.42×10^{-9}	8.26×10^{-8}	6.42×10^{-8}	6.42×10^{-8}	6.42×10^{-8}
0.6	2.08×10^{-7}	2.21×10^{-8}	8.57×10^{-8}	6.46×10^{-8}	6.40×10^{-8}	6.40×10^{-8}
0.7	3.32×10^{-6}	7.34×10^{-8}	8.39×10^{-8}	6.41×10^{-8}	6.38×10^{-8}	6.38×10^{-8}
0.8	4.43×10^{-6}	7.37×10^{-8}	7.71×10^{-9}	6.40×10^{-8}	6.35×10^{-8}	6.35×10^{-8}
0.9	3.97×10^{-6}	2.22×10^{-7}	7.44×10^{-8}	6.40×10^{-8}	6.36×10^{-8}	6.36×10^{-8}
1.0	1.03×10^{-7}	6.49×10^{-9}	9.67×10^{-8}	6.43×10^{-8}	6.35×10^{-8}	6.35×10^{-8}

Table 5. AE assessment of $Q(\xi)$ with the several estimates of M and k.

ξ	Absolute error of GWCM with NDSolve method					
	k=1,M=3	**k=2,M=3**	**k=1,M=4**	**k=2,M=4**	**k=1,M=6**	**k=2,M=6**
0	0	0	0	0	0	0
0.1	3.94×10^{-6}	2.21×10^{-7}	7.84×10^{-8}	5.28×10^{-8}	5.19×10^{-8}	5.19×10^{-8}
0.2	4.39×10^{-6}	6.41×10^{-8}	9.08×10^{-8}	6.76×10^{-8}	6.71×10^{-8}	6.71×10^{-8}
0.3	3.30×10^{-6}	6.22×10^{-8}	8.58×10^{-8}	6.99×10^{-8}	6.92×10^{-8}	6.92×10^{-8}
0.4	2.07×10^{-6}	2.06×10^{-7}	8.28×10^{-8}	6.82×10^{-8}	6.78×10^{-8}	6.78×10^{-8}
0.5	1.57×10^{-6}	6.40×10^{-7}	8.24×10^{-8}	6.40×10^{-8}	6.40×10^{-8}	6.40×10^{-8}
0.6	2.08×10^{-6}	2.21×10^{-8}	8.55×10^{-8}	6.43×10^{-8}	6.38×10^{-8}	6.38×10^{-8}
0.7	3.32×10^{-6}	7.36×10^{-8}	8.37×10^{-8}	6.39×10^{-8}	6.35×10^{-8}	6.35×10^{-8}
0.8	4.43×10^{-6}	7.39×10^{-8}	7.68×10^{-8}	6.38×10^{-8}	6.33×10^{-8}	6.33×10^{-8}
0.9	3.97×10^{-6}	2.22×10^{-7}	7.42×10^{-8}	6.37×10^{-8}	6.34×10^{-8}	6.34×10^{-8}
1.0	1.03×10^{-7}	6.47×10^{-8}	9.65×10^{-8}	6.41×10^{-8}	6.32×10^{-8}	6.32×10^{-8}

Table 6. The numerical results of $S(\xi)$ compared with different methods.

ξ	ND Solve	TWCM	RK4	HATM [9]	AE of HATM	AE of RK4	AE of TWCM
0	300.0000000000	300.000000000	300.00000000	300.000000	0	0	0
0.2	297.5457374954	297.545737502	297.545737498	297.5450103	7.27×10^{-4}	2.60×10^{-7}	6.60×10^{-9}
0.4	294.9667201500	294.966720156	294.966720149	294.9608370	5.88×10^{-3}	9.99×10^{-7}	5.99×10^{-9}
0.6	292.2675486378	292.267548643	292.267548632	292.2474799	2.00×10^{-2}	5.80×10^{-7}	5.19×10^{-9}
0.8	289.4529921276	289.452992132	289.452992119	289.4049390	4.80×10^{-2}	8.60×10^{-7}	4.40×10^{-9}
1.0	286.5279676719	286.527967672	286.527967656	286.4332145	9.47×10^{-2}	1.59×10^{-7}	9.99×10^{-11}

Table 7. The numerical results of $E(\xi)$ compared with different methods.

ξ	ND Solve	TWCM	RK4	HATM [9]	AE of HATM	AE of RK4	AE of TWCM
0	30.00000000000	30.0000000000	30.000000000	30.0000000	0	0	0
0.2	32.43728831577	32.4372879116	32.4372879151	32.43802645	7.38×10^{-4}	4.00×10^{-5}	4.04×10^{-7}
0.4	34.99798599822	34.9979856142	34.9979856209	35.00395898	5.97×10^{-3}	3.77×10^{-5}	3.84×10^{-7}
0.6	37.67742774120	37.6774272634	37.6774272732	37.69779761	2.03×10^{-2}	4.68×10^{-5}	4.78×10^{-7}
0.8	40.47078157756	40.4707810837	40.4707810971	40.51954233	4.87×10^{-2}	4.80×10^{-5}	4.93×10^{-7}
1.0	43.37307052910	43.3730700621	43.3730700785	43.46919314	9.61×10^{-2}	4.50×10^{-5}	4.67×10^{-7}

Table 8. The numerical results of $I(\xi)$ compared with different methods.

ξ	ND Solve	TWCM	RK4	HATM [9]	AE of HATM	AE of RK4	AE of TWCM
0	20.00000000000	20.0000000000	20.000000000	20.0000000	0	0	0
0.2	20.01667577872	20.0166757876	20.0166757876	20.01666441	1.13×10^{-5}	8.88×10^{-7}	8.88×10^{-9}
0.4	20.03469662491	20.0346966341	20.0346966345	20.03460646	9.01×10^{-5}	9.59×10^{-7}	9.19×10^{-9}
0.6	20.05412769437	20.0541277024	20.0541277024	20.05382613	3.01×10^{-4}	8.03×10^{-7}	8.03×10^{-9}
0.8	20.07503159091	20.0750315988	20.0750315988	20.07432344	7.08×10^{-4}	7.89×10^{-7}	7.89×10^{-9}
1.0	20.09746828059	20.0974682885	20.0974682884	20.09609837	1.36×10^{-3}	7.81×10^{-7}	7.91×10^{-9}

Table 9. The numerical results of $R(\xi)$ compared with different methods.

ξ	ND Solve	TWCM	RK4	HATM [9]	AE of HATM	AE of RK4	AE of TWCM
0	65.00000000000	65.0000000000	65.000000000	65.000000	0	0	0
0.2	63.75980401227	63.7598039449	63.7598039449	63.75988658	8.25×10^{-5}	6.73×10^{-6}	6.73×10^{-8}
0.4	62.54229546138	62.5422953933	62.5422953934	62.54295352	6.58×10^{-5}	6.79×10^{-6}	6.80×10^{-8}
0.6	61.34698975500	61.3469896912	61.3469896915	61.34920081	2.21×10^{-3}	6.35×10^{-6}	6.38×10^{-8}
0.8	60.17341134905	60.1734112856	60.1734112856	60.17862847	5.21×10^{-3}	6.34×10^{-6}	7.89×10^{-8}
1.0	59.02109394151	59.0210938786	59.0210938781	59.03123648	1.01×10^{-2}	6.34×10^{-6}	6.29×10^{-8}

Table 10. The numerical results of $Q(\xi)$ compared with different methods.

ξ	ND Solve	TWCM	RK4	HATM [9]	AE of HATM	AE of RK4	AE of TWCM
0	20.00000000000	20.0000000000	20.000000000	20.000000	0	0	0
0.2	21.05185803560	21.0518581028	21.0518581028	21.05177564	8.23×10^{-5}	6.72×10^{-6}	6.72×10^{-8}
0.4	22.08147123480	22.0814713026	22.0814713026	22.08081457	6.56×10^{-5}	6.78×10^{-6}	6.78×10^{-8}
0.6	23.08932315000	23.0893232138	23.0893232138	23.08711678	2.20×10^{-3}	6.38×10^{-6}	6.38×10^{-8}
0.8	24.07588828763	24.0758883509	24.0758883509	24.07068228	5.20×10^{-3}	6.32×10^{-6}	6.32×10^{-8}
1.0	25.04163191445	25.0416319777	25.0416319777	25.03151105	1.01×10^{-2}	6.32×10^{-6}	6.32×10^{-8}

Table 11. **The numerical results of $S(\xi)$ at $\alpha = 0.6$, 0.8 and 0.9.**

ξ	$\alpha = 0.6$		$\alpha = 0.8$		$\alpha = 0.9$	
	TWCM	**HATM**	**TWCM**	**HATM**	**TWCM**	**HATM**
0	300.0000000	300.0000000	300.0000000	300.0000000	300.0000000	300.0000000
0.2	294.7106234	290.8332821	296.3999586	294.2312730	297.0286465	295.9169066
0.4	291.5573732	288.7183111	293.4374249	291.6812730	294.2456359	293.3045941
0.6	288.8582880	286.9466815	290.6279594	289.2823904	291.4708042	290.7063195
0.8	286.4258392	285.3574883	287.8919546	286.9528908	288.6717324	288.0843841
1.0	284.2587780	283.8864707	285.2054067	284.6590141	285.8389362	285.4232667

Table 12. **The numerical results of $E(\xi)$ at $\alpha = 0.6$, 0.8 and 0.9.**

ξ	$\alpha = 0.6$		$\alpha = 0.8$		$\alpha = 0.9$	
	TWCM	**HATM**	**TWCM**	**HATM**	**TWCM**	**HATM**
0	30.00000000	30.00000000	30.00000000	30.00000000	30.00000000	30.00000000
0.2	35.25169464	39.10004523	33.57487590	35.72766190	32.95070893	34.05441224
0.4	38.38080393	41.19892275	36.51577144	38.25886843	35.71371062	36.64785418
0.6	41.05819473	42.95693540	39.30388833	40.63981065	38.46790303	39.22704104
0.8	43.47021513	44.53381791	42.01829081	42.95167533	41.24542858	41.82943376
1.0	45.61813103	45.99336551	44.68280686	45.22800285	44.05565063	44.47046140

Table 13. **The numerical results of $I(\xi)$ at $\alpha = 0.6$, 0.8 and 0.9.**

ξ	$\alpha = 0.6$		$\alpha = 0.8$		$\alpha = 0.9$	
	TWCM	**HATM**	**TWCM**	**HATM**	**TWCM**	**HATM**
0	20.00000000	20.00000000	20.00000000	20.00000000	20.00000000	20.00000000
0.2	20.03706783	20.06569309	20.02473541	20.04041223	20.02028584	20.02820332
0.4	20.06087763	20.08158972	20.04604431	20.05894326	20.03997835	20.04678947
0.6	20.08230238	20.09504715	20.06709651	20.07664739	20.06031743	20.06560725
0.8	20.10249721	20.10721869	20.08842248	20.09406166	20.08157371	20.08488908
1.0	20.12144563	20.11856300	20.11019336	20.11140109	20.10386546	20.10472442

Table 14. The numerical results of $R(\xi)$ at $\alpha = 0.6$, 0.8 and 0.9.

ξ	$\alpha = 0.6$		$\alpha = 0.8$		$\alpha = 0.9$	
	TWCM	**HATM**	**TWCM**	**HATM**	**TWCM**	**HATM**
0	65.00000000	65.00000000	65.00000000	65.00000000	65.00000000	65.00000000
0.2	62.49632797	61.13521917	63.22741744	62.36277835	63.51565943	63.04502340
0.4	61.20269459	60.40677303	61.90801009	61.34428024	62.23613678	61.91386799
0.6	60.17452131	59.82779844	60.74736176	60.44600834	61.04707524	60.86194973
0.8	59.30331456	59.33049050	59.68779443	59.62275299	59.92104120	59.86504614
1.0	58.59233755	58.88735002	58.70747394	58.85433742	58.84566295	58.91180471

Table 15. The numerical results of $Q(\xi)$ at $\alpha = 0.6$, 0.8 and 0.9.

ξ	$\alpha = 0.6$		$\alpha = 0.8$		$\alpha = 0.9$	
	TWCM	**HATM**	**TWCM**	**HATM**	**TWCM**	**HATM**
0	20.00000000	20.00000000	20.00000000	20.00000000	20.00000000	20.00000000
0.2	22.11751690	23.25119176	21.50176424	22.22707314	21.25832669	21.65432952
0.4	23.20408274	23.85718191	22.61455672	23.08151053	22.33908977	22.60713914
0.6	24.06413397	24.33723469	23.58978058	23.83245361	23.34006118	23.49023543
0.8	24.79016955	24.74838860	24.47693785	24.51838248	24.28486364	24.32434237
1.0	25.37928523	25.11379385	25.29486272	25.15651828	25.18422414	25.11921053

6. Conclusion

In the present work, we have provided the numerical approximation of the PWD model. The TWCM with the Caputo fractional derivative is used to generate the numerical solution. We can apply the scheme to other types of fractional derivatives, such as Riemann-Liouville, Caputo-Fabrizio, Mittag-Leffler, and Atangana-Baleanu fractional derivatives. A novel operational matrix is constructed based on the Taylor wavelets at diverse resolutions (k) and incorporated into the collocation method. Methods like HATM, RK4, and ND Solver have been compared with the results obtained from the established technique. Since the suggested technique is more precise than the current numerical approaches in use, the findings in the tables and figures support this claim. Numerical examples support the idea that only a small number of TWBs are required to achieve appropriate results. The above statement emphasizes our belief that the method efficiently deals with highly nonlinear FDEs. This approach is straightforward, easy to apply, and requires less computing power. Thus, compared with RK4 and HATM, we deduced that the technique under discussion is a helpful tool for obtaining the numerical approximation of the mathematical models in the form of nonlinear FDEs. Further, by slightly modifying the method, the Taylor wavelet method can solve the PDEs, higher-order systems of ordinary differential equations, stiff systems, delay differential equations, and chemical and biological models.

Declarations

Availability of Data and Materials: The data supporting this study's findings are available within the article.
Competing interests: The authors declare that they have no competing interests.
Author's contributions: KS proposed the main idea of this paper. KS and MG prepared the manuscript and performed all the steps of the proofs in this research. Both authors contributed equally and significantly to writing this paper. Both authors read and approved the final manuscript.
Conflict of interest: The author declares no conflict of interest.
Funding: The author states that no funding is involved.

Acknowledgements

The author expresses his affectionate thanks to the DST-SERB, Govt. of India, New Delhi for the financial support under Empowerment and Equity Opportunities for Excellence in Science for 2023-2026. F.No.EEQ/2022/620 Dated:07/02/2023.

References

[1] K. Tomoya, and Y. Tokushige., *Inoculation experiments of a nematode, Bursaphelenchus sp., onto pine trees*, Journal of the Japanese Forestry Society, 1971, 53(7), 210–218.

[2] M. Yasuharu, and T. Kiyohara, *Description of Bursaphelenchus lignicolus n. sp.(Nematoda: Aphelenchoididae) from pine wood and histopathology of nematode-infested trees*, 1972, 120–124.

[3] S. Kamal, M. A. Alqudah, F. Jarad, and T. Abdeljawad, *Semi-analytical study of Pine Wilt Disease model with convex rate under Caputo-Febrizio fractional order derivative*, Chaos, Solitons and Fractals, 2020, 135, 109754.

[4] M. Yasuharu, *Pathology of the pine wilt disease caused by Bursaphelenchus xylophilus*, 1983, 201–220.

[5] M. Yasuharu, *History of pine wilt disease in Japan*, Journal of nematology, 1988, 20(2), 219.

[6] F. Kenji, *Physiological process of the symptom development and resistance mechanism in pine wilt disease*, Journal of forest research, 1997, 2(3), 171–181.

[7] P. Diogo, G. Grass, and P. V. Morais, *Understanding pine wilt disease: roles of the pine endophytic bacteria and of the bacteria carried by the disease-causing pinewood nematode*, MicrobiologyOpen, 2017, 6(2), e00415.

[8] O. Muhammad, T. Hussain, A. U. Awan, A. Aslam, R. A. Khan, F. Ali, and F. Tasneem, *Bio-inspired analytical heuristics to study pine wilt disease model*, Scientific reports, 2020, 10(1), 3534.

[9] V. Padmavathi, N. Magesh, K. Alagesan, M. I. Khan, S. Elattar, M. Alwetaishi, and A. M. Galal, *Numerical modeling and symmetry analysis of a pine wilt disease model using the Mittag-Leffler kernel*, Symmetry, 2022, 14(5), 1067.

[10] A. U. Awan, A. Ullah, M. Ozair, Q. Din, and T. Hussain, *Stability analysis of pine wilt disease model by periodic use of insecticides*, Journal of Biological Dynamics, 2016, 10(1), 506–524.

[11] L. Yongjin, F. Haq, K. Shah, M. Shahzad, and G. ur Rahman, *Numerical analysis of fractional order Pine wilt disease model with bilinear incident rate*, Journal of Mathematics and Computer Science, 2017, 17, 420–428.

[12] A. M. El-Sayed, S. Z. Rida, and Y. A. Gaber. *On the stability analysis and solutions of fractional order pine wilt disease model*, Applied Mathematics and Information Sciences, 2020, 14(6), 1137–1146.

[13] H. Takasar, A. Aslam, M. Ozair, F. Tasneem, and J. F. G. Aguilar, *Dynamical aspects of pine wilt disease and control measures*, Chaos, Solitons and Fractals, 2021, 145, 110764.

[14] L. K. Sung, and A. A. Lashari, *Global Stability of a Host-Vector Model for Pine Wilt Disease with Nonlinear Incidence Rate*, In Abstract and Applied Analysis, 2014, 1, 219173.

[15] L. K. Sung, and A. A. Lashari. *Stability analysis and optimal control of pine wilt disease with horizontal transmission in vector population*, Applied Mathematics and Computation, 2014, 226, 793–804.

[16] S. Kumbinarasaiah, and K. R. Raghunatha, *The applications of the Hermite wavelet method to nonlinear differential equations arising in heat transfer*, International Journal of Thermofluids, 2021 9, 100066.

[17] S. Kumbinarasaiah, and R. A. Mundewadi, *Numerical solution of fractional-order integro-differential equations using the Laguerre wavelet method*, Journal of Information and Optimization Sciences, 2022, 43(4), 643–662.

[18] M. Faheem, A. Raza, and A. Khan, *Collocation methods based on Gegenbauer and Bernoulli wavelets for solving neutral delay differential equations*, Mathematics and Computers in Simulation, 2021, 180, 72–92.

[19] L. Fei, H. M. Baskonus, S. Kumbinarasaiah, G. Manohara, W. Gao, and E. Ilhan, *An efficient numerical scheme for biological models in the frame of Bernoulli wavelets*, Computer Modelling in Engineering and Sciences, 2023, 137, 3.

[20] D. Sharanjeet, J. A. T. Machado, D. W. Brzezinski, and M. S. Osman, *A Chebyshev wavelet collocation method for some types of differential problems*, 2021, Symmetry 13(4), 536.

[21] S. Kumbinarasaiah, *Hermite wavelets approach for the multi-term fractional differential equations*, Journal of Interdisciplinary Mathematics, 2021, 24(5), 1241–1262.

[22] S. Kumbinarasaiah, and A. Waleed, *Hermite wavelet method for solving nonlinear Rosenau-Hyman equation*, Partial Differential Equations in Applied Mathematics, 2021, 4, 100062.

[23] L. Xinxiu, *Numerical solution of fractional differential equations using cubic B-spline wavelet collocation method*, Communications in Nonlinear Science and Numerical Simulation, 2012, 17(10), 3934–3946.

[24] L. I. Yuanlu, *Solving a nonlinear fractional differential equation using Chebyshev wavelets*, Communications in Nonlinear Science and Numerical Simulation, 2010, 15(9), 2284–2292.

[25] I. Abdulnasir, and C. Phang, *Genocchi wavelet-like operational matrix and its application for solving non-linear fractional differential equations*, Open Physics, 2016, 14(1), 463–472.

[26] E. Keshavarz, Y. Ordokhani, and M. Razzaghi, *Bernoulli wavelet operational matrix of fractional order integration and its applications in solving the fractional order differential equations*, Applied Mathematical Modelling, 2014, 38(24), 6038–6051.

[27] S. Kumbinarasaiah, G. Manohara, and G. Hariharan, *Bernoulli wavelets functional matrix technique for a system of nonlinear singular Lane Emden equations*, Mathematics and Computers in Simulation, 2022, 204, 133–165.

[28] S. Kumbinarasaiah, and G. Manohara, *Modified Bernoulli wavelets functional matrix approach for the HIV infection of CD4+ T cells model*, Results in Control and Optimization, 10, 100197.

[29] A. Thabet, R. Amin, K. Shah, Q. Al-Mdallal, and F. Jarad, *Efficient sustainable algorithm for numerical solutions of systems of fractional order differential equations by Haar wavelet collocation method*, Alexandria Engineering Journal, 2020, 59(4), 2391–2400.

[30] E. Sertac, A. Demir, and E. Ozbilge, *Solving inverse non-linear fractional differential equations by generalized Chelyshkov wavelets*, Alexandria Engineering Journal, 2023, 66, 947–956.

[31] G. Manohara, and S. Kumbinarasaiah, *Fibonacci wavelet collocation method for the numerical approximation of fractional order Brusselator chemical model*, Journal of Mathematical Chemistry, 2023, 1–31.

[32] G. Manohara, and S. Kumbinarasaiah, *Fibonacci wavelets operational matrix approach for solving chemistry problems*, Journal of Umm Al-Qura University for Applied Sciences, 2023, 1–18.

[33] M. Fakhrodin, and C. Cattani, *A generalized fractional-order Legendre wavelet Tau method for solving fractional differential equations*, Journal of Computational and Applied Mathematics, 2018, 339, 306–316.

[34] R. Mujeeb, and U. Saeed, *Gegenbauer wavelets operational matrix method for fractional differential equations*, Journal of the Korean Mathematical Society, 2015, 52(5), 1069–1096.

[35] D. Idris, A. Canivar, and A. Sahin, *Taylor-Galerkin and Taylor-collocation methods for the numerical solutions of Burgers equation using B-splines*, Communications in Nonlinear Science and Numerical Simulation, 2011, 16(7), 2696–2708.

[36] E. Keshavarz, Y. Ordokhani, and M. Razzaghi, The Taylor wavelets method for solving the initial and boundary value problems of Bratu-type equations. Applied Numerical Mathematics, 2018, 128, 205–216.

[37] G. Sevin, *Taylor wavelet solution of linear and nonlinear Lane-Emden equations*, Applied Numerical Mathematics, 2020, 158, 44–53.

[38] P. T. Toan, T. N. Vo, and M. Razzaghi, *Taylor wavelet method for fractional delay differential equations*, Engineering with Computers, 2021, 37(1), 231–240.

[39] S. C. Shiralashetti, and S. I. Hanaji, *Taylor wavelet collocation method for Benjamin-Bona-Mahony partial differential equations*, Results in Applied Mathematics, 2021, 9, 100139.

[40] T. N. Vo, M. Razzaghi, and P. T. Toan, *Fractional-order generalized Taylor wavelet method for systems of nonlinear fractional differential equations with application to human respiratory syncytial virus infection*, Soft Computing, 2022, 26(1), 165–173.

[41] S. Kumbinarasaiah, *A novel approach for multi-dimensional fractional coupled Navier-Stokes equation*, SeMA Journal, 2022, 1–22.

[42] S. Sedigheh, Y. Ordokhani, and S. A. Yousefi, *Fibonacci wavelets and their applications for solving two classes of time-varying delay problems*, Optimal Control Applications and Methods, 2020, 41(2), 395–416.

[43] Y. Li, S. Kumbinarasaiah, G. Manohara, H. M. Baskonus, and C. Cattani, *Numerical solution of fractional PDEs through wavelet approach*, Zeitschrift für angewandte Mathematik und Physik, 2024, 75(2), 61.

[44] L. K. Sung, and A. A. Lashari, *Stability analysis and optimal control of pine wilt disease with horizontal transmission in vector population*, Applied Mathematics and Computation, 2014, 226, 793–804.

[45] G. Manohara, and S. Kumbinarasaiah, *Numerical solution of some stiff systems arising in chemistry via Taylor wavelet collocation method*, Journal of Mathematical Chemistry, 2024, 62(1), 24–61.

[46] K. Aasma, A. Rehan, K. S. Nisar, and M. S. Osman, *Splines solutions of boundary value problems that arises in sculpturing electrical process of motors with two rotating mechanism circuit*, Physica Scripta, 2021, 96(10), 104001.

[47] G. Manohara, and S. Kumbinarasaiah, *An innovative Fibonacci wavelet collocation method for the numerical approximation of Emden-Fowler equations*, Applied Numerical Mathematics, 2024, 201, 347–369.

[48] R. Saima, K. T. Kubra, S. Sultana, P. Agarwal, and M. S. Osman, *An approximate analytical view of physical and biological models in the setting of Caputo operator via Elzaki transform decomposition method*, Journal of Computational and Applied Mathematics, 2022, 413, 114378.

[49] Q. Sania, A. Soomro, E. Hincal, J. R. Lee, C. Park, and M. S. Osman, *An efficient variable stepsize rational method for stiff, singular and singularly perturbed problems*, Alexandria Engineering Journal, 2022, 61(12), 10953–10963.

[50] K. Sunil, R. P. Chauhan, M. S. Osman, and S. A. Mohiuddine, *A study on fractional HIV-AIDs transmission model with awareness effect*, Mathematical Methods in the Applied Sciences, 2023, 46(7), 8334–8348.

[51] G. Manohara, and S. Kumbinarasaiah, *Numerical approximation of fractional SEIR epidemic model of measles and smoking model by using Fibonacci wavelets operational matrix approach*, Mathematics and Computers in Simulation, 2024, 221, 358–396.

[52] A. O. Abu, S. Tayebi, D. Baleanu, M. S. Osman, W. Mahmoud, and H. Alsulami, *A numerical combined algorithm in cubic B-spline method and finite difference technique for the time-fractional nonlinear diffusion wave equation with reaction and damping terms*, Results in Physics, 2022, 41, 105912.

[53] S. Lei, S. Tayebi, O. A. Arqub, M. S. Osman, P. Agarwal, W. Mahamoud, M. Abdel-Aty, and M. Alhodaly. *The novel cubic B-spline method for fractional Painleve and Bagley-Trovik equations in the Caputo, Caputo-Fabrizio,*

and conformable fractional sense, Alexandria Engineering Journal, 2023, 65, 413–426.

[54] K. Aasma, A. S. A Alsubaie, M. Inc, A. Rehan, W. Mahmoud, and M. S. Osman, *Cubic splines solutions of the higher order boundary value problems arise in sandwich panel theory*, Results in Physics, 2022, 39, 105726.

[55] G. Manohara, and S. Kumbinarasaiah, *Numerical approximation of the typhoid disease model via the Genocchi wavelet collocation method*, Journal of Umm Al-Qura University for Applied Sciences, 2024, 1–16.

[56] Q. Sania, M. A. Akanbi, A. A. Shaikh, A. S. Wusu, O. M. Ogunlaran, W. Mahmoud, and M. S. Osman, *A new adaptive nonlinear numerical method for singular and stiff differential problems*, Alexandria Engineering Journal, 2023, 74, 585–597.

[57] I. M. Ashik, A. H. Ganie, M. M. Miah, and M. S. Osman, *Extracting the ultimate new soliton solutions of some nonlinear time fractional PDEs via the conformable fractional derivative*, Fractal and Fractional, 2024, 8(4), 210.